

Copyright Warning & Restrictions

The copyright law of the United States (Title 17, United States Code) governs the making of photocopies or other reproductions of copyrighted material.

Under certain conditions specified in the law, libraries and archives are authorized to furnish a photocopy or other reproduction. One of these specified conditions is that the photocopy or reproduction is not to be “used for any purpose other than private study, scholarship, or research.” If a user makes a request for, or later uses, a photocopy or reproduction for purposes in excess of “fair use” that user may be liable for copyright infringement,

This institution reserves the right to refuse to accept a copying order if, in its judgment, fulfillment of the order would involve violation of copyright law.

Please Note: The author retains the copyright while the New Jersey Institute of Technology reserves the right to distribute this thesis or dissertation

Printing note: If you do not wish to print this page, then select “Pages from: first page # to: last page #” on the print dialog screen

The Van Houten library has removed some of the personal information and all signatures from the approval page and biographical sketches of theses and dissertations in order to protect the identity of NJIT graduates and faculty.

ABSTRACT

FABRICATION OF INTEGRATED OPTIC SENSOR TO MONITOR POLLUTANT CONCENTRATION IN EFFLUENTS

by
Kiran V Chatty

An attempt has been made to fabricate an integrated optic sensor to monitor pollutant concentration in effluents. Optic fiber has to be coupled to the waveguide in order to send light through the waveguide. In order to facilitate the easy coupling of the fiber to the waveguide, V-grooves were formed in the silicon substrate. In order to achieve this Silicon nitride was deposited to serve as an etch mask. An attempt was made to obtain low stress silicon nitride films.

This work also attempted to synthesize the materials required to fabricate the waveguide. LPCVD processes were developed to produce undoped and Phosphorus doped SiO₂ films. Undoped SiO₂ is used as a cladding material for waveguide. The Phosphorus doped SiO₂ (PSG) is the core material of the waveguide. Diethylsilane (DES) was used as a precursor for the deposition of the undoped oxide and Trimethylphosphite (TMP) was used as the Phosphorus source for the deposition of the PSG films. Conditions for dry etching of SiO₂ and PSG was developed.

**FABRICATION OF INTEGRATED OPTIC SENSOR TO MONITOR
POLLUTANT CONCENTRATION IN EFFLUENTS**

by
Kiran Chatty

**A Thesis
Submitted to the faculty of
New Jersey Institute of Technology
in Partial Fulfillment of the Requirements for the Degree of
Master of science in Engineering Science**

Interdisciplinary Program in Materials Science and Engineering


October 1996

APPROVAL SHEET

Fabrication of Integrated Optic Sensor
to Monitor Pollutant Concentration in Effluents

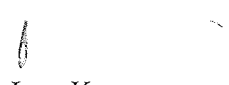
Kiran V Chatty

Thesis & Abstract Approved
by the Examining Committee


Dr. Roland A. Levy, Advisor

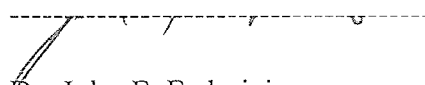

Date

Department of Physics


Dr. Lev Krasnaperov


Date

Department of Chemistry


Dr. John F. Federici


Date

Department of Physics

New Jersey Institute of Technology, Newark, New Jersey

BIOGRAPHICAL SKETCH

Author: Kiran V Chatty
Degree: Master of Science
Date: October 1996

Undergraduate and Graduate Education:

- Master of Science in Engineering Science
New Jersey Institute of Technology
Newark, NJ, 1996
- Bachelor of Technology in Electrochemical Engineering
Central Electrochemical Research Institute (CECRI)
Karakkudi, India, 1995

Major: Materials Science and Engineering

Professional Experience

Research Assistant CVD laboratory, NJIT 1995-1996

**This thesis is dedicated to
my parents**

ACKNOWLEDGMENT

I would like to express my sincere gratitude to my advisor, Professor Roland A Levy for his guidance, inspiration, and support throughout this research.

Special thanks to Professor Lev Krasnaperov, Professor John F.Federici for serving as members of the thesis review committee.

I would like to thank Dr. Jan Opyrchal and Vital Sigal, for their help and guidance.

I would like to thank my late friend Manish for his suggestions and constant encouragement that he provided me throughout the course of study at NJIT. I would also like to thank the other CVD lab members including, Romiana Petrova, Mahalingam Bhaskaran, Chenna Ravindranath, Vijayalakshmi Venkatesan, Sung Jun Lee.

TABLE OF CONTENTS

Chapter	Page
1 INTRODUCTION.....	1
1.1 Chemical Vapor Deposition.....	2
1.1.1 Fundamental Aspects of CVD.....	3
1.1.2 Transport Phenomena of CVD.....	4
1.1.3 Film Growth Aspects of CVD.....	6
1.2 Low Pressure CVD Process.....	7
1.2.1 Mechanism.....	8
1.2.2 Factors Affecting Film Uniformity.....	8
1.3 Advantages of CVD.....	9
1.4 Limitations of CVD.....	10
1.5 Mach Zehnder Interferometer.....	10
1.6 V-Grooves.....	12
1.7 Lithography.....	12
1.7.1 Introduction.....	12
1.7.2 Basic Photoresist Terminology.....	15
1.8 Etching.....	16
1.8.1 Terminology of Etching.....	16
1.8.2 Wet Etching of Technology.....	18
1.8.3 Dry Etching of Technology.....	20

TABLE OF CONTENTS
(Continued)

Chapter	Page
2 REVIEW OF LITERATURE.....	23
2.1 Introduction.....	23
2.2 Deposition Techniques.....	23
2.2.1 Deposition Techniques.....	24
2.2.2 Properties of Films Deposited using DES.....	26
2.3 LPCVD of Phosphosilicate Glass.....	27
2.4 CVD of Silicon Nitride.....	28
2.5 Mach Zehnder Interferometer.....	29
3 EXPERIMENTAL PROCEDURE.....	31
3.1 Flow Sheet for the Fabrication of Mach Zehnder Interferometer.....	31
3.2 Deposition of Thermal Oxide.....	33
3.2.1 Introduction.....	33
3.2.2 Deposition Procedure.....	34
3.3 Deposition of Silicon Nitride.....	34
3.3.1 Introduction.....	34
3.3.2 Description of LPCVD Reactor.....	36
3.3.3 Deposition Procedure.....	36
3.3.4 Experimental Details.....	37
3.4 Deposition of SiO ₂ by LPCVD.....	38

TABLE OF CONTENTS
(Continued)

Chapter	Page
3.4.1 Introduction.....	38
3.4.2 LPCVD Reactor.....	39
3.4.3 Leakage Check.....	40
3.4.4 Calibration of Gas Flow System.....	41
3.5 Deposition Procedure.....	43
3.5.1 Experimental Details.....	44
3.6 Photolithography.....	47
3.6.1 Introduction.....	47
3.6.2 Description of Lithographic Process.....	47
3.7 Reactive Ion Etching.....	49
3.7.1 Introduction.....	49
3.7.2 Description of Reactor for RIE.....	49
3.7.3 Description of RIE Process.....	50
3.8 Etching of Wafers in 49% KOH.....	51
3.9 Stripping of Silicon Nitride.....	52
4 RESULTS AND DISCUSSION.....	54
4.1 Introduction.....	54
4.2 LPCVD of Silicon Nitride.....	54
4.2.1 Reactive Ion Etching of Silicon Nitride.....	56

TABLE OF CONTENTS
(Continued)

Chapter	Page
4.3 LPCVD of SiO ₂ and PSG.....	56
4.3.1 FTIR Analysis of SiO ₂	56
4.3.2 FTIR Analysis of PSG.....	58
4.3.2.1 Determination of P Content.....	60
4.4 Wet Etching of Wafers in KOH.....	62
5 CONCLUSIONS.....	63
REFERENCES.....	65

LIST OF TABLES

Table		Page
2.1	New precursors of CVD SiO ₂	25
2.2	Properties of DES.....	26
2.3	Properties of Silicon Nitride.....	28
3.1	Conditions for deposition of Boron Nitride.....	35
3.2	The conditions for deposition of silicon carbide.....	35
3.3	Conditions for deposition of silicon nitride.....	37
3.4	Specifications of the Si wafer.....	43
3.5	Conditions for deposition of SiO ₂	44
3.6	Conditions for etching of Silicon nitride.....	50
3.7	Conditions for etching SiO ₂	52

LIST OF FIGURES

Figure	Page
1.1 Deposition rate as a function of substrate temperature exemplifying diffusion controlled and surface-reaction regimes.....	6
1.2 Optic fiber in a V groove etched anisotropically in silicon substrate.....	13
1.3 Anisotropic etch profile.....	18
3.1 Schematic Representation of LPCVD reactor.....	39
4.1 Plot of Stress of Silicon Nitride vs NH ₃	55
4.2 FTIR spectrum of Silicon dioxide deposited at 475°C.....	57
4.3 FTIR spectrum of PSG film.....	59
4.4 Etch rates of Silicon dioxide and P-glass films in P-etch solution.....	60
4.5 Comparison of P=O peaks after the film is exposed to atmosphere for 5 months.....	61

CHAPTER 1

INTRODUCTION

Environmental monitoring has become a major concern as society begins to deal with its air and water pollution problems. To address these issues, environmental samples are currently collected and analyzed for a large number of substances such as aromatic hydrocarbons, organic chlorides, phenols, and organophosphates. Although effective, the cost of manual sample collection prohibits optimal usage. This shortcoming warrants development of remote monitoring equipment.

In the recent past work is being done to monitor the pollutants by optical techniques. These remote sensing methods use optical fibers or a combination of fiber coupling and a planar waveguide sensing device. An attempt is made here to fabricate an optical waveguide sensor called an integrated optic sensor (Mach Zehnder interferometer) for remotely monitoring pollutants of interest.

The operation of the sensor is based on the detection of changes in the refractive index from baseline water value due to the presence of pollutants. These changes are measured by exposing one arm of a symmetric Mach-Zehnder interferometer to the contaminated liquid while the other reference arm is being protected by a glass buffer layer. The interferometric output can be calculated as a function of arm length and index difference between the reference and the active arm. This device has been designed so as to be mass produced using standard silicon based processes. The sensor system is

analyses of contaminants in water systems. In order to achieve the primary aim of this study, fabrication of the optic sensor, work was done to deposit SiO₂, P-Glass, boron nitride, silicon carbide, silicon nitride films, characterize these films and optimize deposition parameters to obtain low stress and other desired properties in the films.

1.1 Chemical Vapor Deposition

Chemical Vapor Deposition (CVD) is one of the most important methods of film formation used in the fabrication of very large scale integrated (VLSI) silicon circuits, as well as of microelectronic solid state devices in general. In this process, chemicals in the gas or vapor phase are reacted at the surface of the substrate where they form a solid product. A large variety of materials, practically all those needed in microelectronic device technology, can be created by CVD. These materials comprise insulators and dielectrics, elemental and compound semiconductors, electrical conductors, superconductors and magnetics. In addition to its unique versatility, this materials synthesis and vapor phase growth method can operate efficiently at relatively low temperatures. For example, refractory oxide glasses and metals can be deposited at temperatures of only 300° to 500°C. This feature is very important in advanced VLSI devices with short channel lengths and shallow junctions, where lateral and vertical diffusion of the dopants must be minimized. This also helps in minimizing process-induced crystallographic damage, wafer warpage and contamination by diffusion of impurities.

1.1.1 Fundamental Aspects of CVD

Chemical vapor deposition is defined as a process whereby constituents of the gas or vapor phase react chemically near or on the substrate surface to form a solid product. This product can be in the form of a thin film, a thick coating, or if allowed to grow, a massive bulk. It can have a single-crystalline, poly-crystalline, or amorphous structure. Chemical and physical conditions during the deposition reaction can strongly affect the composition and structure of the product. This deposition technology has become one of the most means of creating thin films and coatings in solid state microelectronics where some of the most sophisticated purity and composition requirements must be met.

Chemical reaction type basic to CVD include pyrolysis, oxidation, reduction, hydrolysis, nitride and carbide formation, synthesis reactions and chemical transport. A sequence of several reaction types may be involved to create a particular end product. The chemical reactions may take place not only on the substrate surface (heterogeneous reaction), but also in the gas phase (homogeneous reaction). Heterogeneous reactions are much more desirable, as such reactions selectively occur only on the heated surfaces, and produce good quality films. Homogeneous reactions, on the other hand are undesirable, as they form gas phase clusters of the depositing material, which will result in poor adherence, low density or defects in the film. Thus one important characteristic of CVD application is the degree to which heterogeneous reactions are favored over homogeneous reactions. This film could be a thin film or a thick coating and should be less volatile to remain on the substrate.

1.1.2 Transport Phenomena of CVD

CVD of the film is almost always a heterogeneous reaction. The sequence of the steps in the usual heterogeneous processes can be described as follows:

1. Arrival of the reactants

- a. bulk transport of reactants into the chamber,
- b. gaseous diffusion of reactants to the substrate surface,
- c. adsorption of reactants onto the substrate surface.

2. Surface chemistry

- a. surface diffusion of reactants,
- b. surface reaction.

3. Removal of by-products

- a. desorption of by-products from the substrate surface,
- b. gaseous diffusion of by-products away from the substrate surface,
- c. bulk transport of by-products out of the reaction chamber.

The steps are sequential and the slowest process is the rate determining step.

The sequential steps of deposition process can be grouped into (i) mass transport-limited regime and (ii) surface-reaction-limited regime. If the deposition process is limited by the mass transfer, the transport process occurred by the gas-phase diffusion is proportional to the diffusivity of the gas and the concentration gradient. The mass transport process which limits the growth rate is only weakly dependent on temperature. On the other hand, it is very important that the same concentration of reactants be present in the bulk gas regions adjacent to all locations of a wafer, as the arrival rate is directly

proportional to the concentration in the bulk gas. Thus, to ensure films of uniform thickness, reactors which are operated in the mass-transport-limited regime must be designed so that all locations of wafer surfaces and all wafers in a run are supplied with an equal flux of reactant species.

If the deposition process is limited by the surface reaction, the growth rate, R , of the film deposited can be expressed as $R = R_0 \cdot \exp(-E_a/RT)$, where R_0 is the frequency factor, E_a is the activation energy - usually 25-100 kcal/mole for surface process, R is the gas constant, and T , the absolute temperature. In the operating regime, the deposition rate is a strong function of the temperature and an excellent temperature control is required to achieve the film thickness uniformity that is necessary for controllable integrated circuit fabrication.

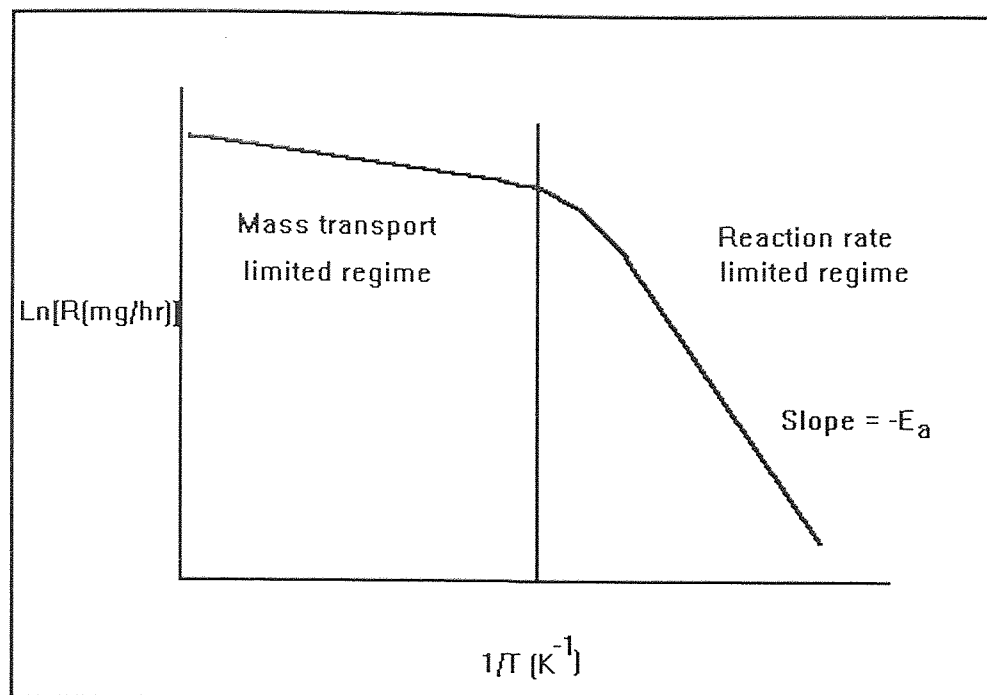


Figure 1.1 Deposition rate as a function of substrate temperature exemplifying diffusion controlled and surface-reaction controlled regimes

On the other hand, under such conditions the rate at which reactant species arrive at the surface is not as important. Thus, it is not as critical that the reactor be designed to supply an equal flux of reactants to all locations of the wafer surface. It will be seen that in horizontal low pressure CVD reactors, wafers can be stacked vertically and at very close spacing because such systems operate in a surface-reaction-rate limited regime. In deposition processes that are mass-transport limited, however, the temperature control is not nearly as critical. As shown in Figure 1.1, a relatively steep temperature range, and a milder dependence in the upper range, indicating that the nature of the rate-controlling step changes with temperature.

1.1.3 Film Growth Aspects of CVD

In general, lower temperature and higher gas phase concentration favor formation of polycrystalline deposits. Under these conditions, the arrival rate at the surface is high, but the surface mobility of adsorbed atoms is low. Many nuclei of different orientation are formed, which upon coalescence result in a film consisting of many differently oriented grains. Further decrease in temperature and increase in supersaturation result in even more nuclei, and consequently in finer-grained films, eventually leading to the formation of amorphous films when crystallization is completely prevented. Amorphous films include oxides, nitrides, carbides and glasses are of great technical importance for microelectronics applications.

Deposition variables such as temperature, pressure, input concentrations, gas flow rates, reactor geometry and reactor opening principle determine the deposition rate and the properties of the film deposit.

1.2 Low Pressure CVD Process

The most important and widely used CVD processes are atmospheric pressure CVD (APCVD), low pressure CVD (LPCVD) and plasma enhanced CVD (PECVD). Only LPCVD is discussed in detail below as this process is employed in this study.

Most low pressure CVD processes are conducted by resistance heating and less frequently infrared radiation heating techniques to attain isothermal conditions so that the substrate and the reactor walls are of similar temperature. The deposition rate and

uniformity of the films created by all CVD processes are governed by two basic parameters (i) the rate of mass transfer of reactant gases to the substrate surface and (ii) the rate of surface reaction of the reactant gases at the substrate surface. Lowering the pressure to below atmospheric pressure enhances the mass transfer rate relative to the surface reaction rate thus making it possible to deposit films uniformly in a highly economical close spaced positioning of the substrate wafers in the standup position.

1.2.1 Mechanism

The mass transfer of the gases involve their diffusion across a slowly moving boundary layer adjacent to the substrate surface. The thinner this boundary layer and the higher the gas diffusion rate, the greater is the mass transport that results. Surface reaction rates, on the other hand, depend mainly upon reactant concentration and deposition temperature. High deposition rates are attainable with LPCVD despite the fact that the operating total pressure is usually two to four orders of magnitude lower than atmospheric CVD. This is due to the fact that the large mole fraction of reactive gases in LPCVD, and no or little diluent gas is required. Wafer spacing has a marked effect on the deposition rate of all types of films, the deposition rate increasing linearly with increasing spacing since the quantity of available reactant per wafer increases.

1.2.2 Factors Affecting Film Uniformity

Some of the main factors affecting the film thickness uniformity in LPCVD are the temperature profile in the reactor, the pressure level in the reactor and the reactant gas flow rates. To obtain a flat thickness profile across each substrate wafer throughout the

reactor requires a judicious adjustments of these parameters. In tubular reactors, increase in temperature or pressure, increases the deposition rate upstream, thereby using up more reactant gases and leaving less to react at the downstream end; the opposite effect takes place on lowering the temperature and pressure. Similar effects occur with variations of the reactant gas flow rates at constant gas partial pressure, or with changes in the size and number of the wafers processed per deposition run. The uniformity of thickness and step coverage of these films are very good. These films have fewer defects, such as particulate contaminants and pinholes, because of their inherently cleaner hot wall operations and the vertical wafer positioning that minimize the formation and codeposition of homogeneously gas phase nucleated particulates.

1.3 Advantages of CVD

Thin films are used in a host of applications in VLSI fabrication, and can be synthesized by a variety of techniques. Regardless of the method by which they are formed, however, the process must be economical, and the resultant films must exhibit uniform thickness, high purity and density, controllable composition and stoichiometries, high degree of structural perfection, excellent adhesion and good step coverage. CVD processes are often selected over competing deposition techniques because they offer the following advantages:

1. A variety of stoichiometric and non stoichiometric compositions can be deposited by accurate control of process parameters.

2. High purity films can be deposited that are free from radiation damage without further processing.
3. Results are reproducible.
4. Uniform thickness' can be achieved by low pressures.
5. Conformal step coverage can be obtained.
6. Selective deposition can be obtained with proper design of the reactor.
7. The process is very economical because of its high throughput and low maintenance costs.

1.4 Limitations of CVD

Fundamental limitations of CVD are the chemical reaction feasibility and the reaction kinetics that govern the CVD processes. Technological limitations of CVD include the unwanted and possibly deleterious but necessary by-products of reaction that must be eliminated, and the ever present particle generation induced by homogeneous gas phase nucleation that must be minimized.

1.5 Mach Zehnder Interferometer

This optical sensor under investigation, consists of a symmetric, single mode Mach-Zehnder interferometer with one arm exposed directly to the contaminated water. A glass buffer layer protects the reference arm from the influence of pollutants. Laser light is coupled into the waveguide and split into the reference and sampling arms using a Y-splitter configuration. When the active arm is exposed to pollutant molecules, there is an

effective change in the refractive index sampled by that arm. Thickness changes can also occur in any hydrophobic layer which adheres to the coated arm affecting the refractive index sampled by that arm. Therefore, a phase difference, $\Delta\Phi$, develops between the active and reference arm. When light from the two interferometer arms recombine, constructive or destructive interference occurs and the light intensity exiting the interferometer, I_x , ratioed to input light, I_o , is given by :

$$I_x/I_o = 1/2 (1 + \cos \Delta\Phi)$$

where

$$\Delta\Phi = 2\pi L(n_2 - n_1)/\lambda_o$$

with L being the common length for both arms of the interferometer, n_i the effective index of arm i , and λ_o is the input light wavelength. Therefore, the phase difference is directly proportional to the effective index difference

($\Delta n_{\text{eff}} = n_2 - n_1$) between the waveguide arms. Since the pollutant level affects Δn_{eff} , then the interferometer's output intensity changes with the concentration of pollution present in the sample.

An important advantage of this sensor is its size. The distance between the interferometer's arms is on the order of 0.1 mm while the length of the interferometer is on the order of 1 cm. By placing numerous interferometers parallel to each other with different coatings, the resultant device can be made to measure the concentration of different pollutant species simultaneously. The area of the device occupies an area no bigger than a thumb nail. Another advantage to this approach is the compatibility of the technology with standard silicon-based processing where photolithography and chemical

etching steps can be used to mass produce copies of the pattern at a cost of less than a dollar per chip. For a typical arm length $L = 0.6$ cm, and a $\lambda_0 = 633$ nm, $\Delta\Phi = \pi$ (i.e., 1 fringe shift or 100% signal modulation) for a $\Delta n_{\text{eff}} = 6 \times 10^{-5}$. Therefore, extremely small changes in the effective index, caused by low concentrations of pollutants in the water, can be measured using this interferometric approach.

1.6 V Grooves

The optical and physical connection of optical fibers to optoelectronic devices is an essential part of telecommunications technology. Interconnects must provide precise alignment and good mechanical connection for the lifetime of the device. Single mode optical fibers have small diameter cores (~ 9 μm or less) that require precise alignment with optical detectors and modulators. Movement of the core with respect to the detector, induced by thermal or vibrational effects, for example may lead to signal losses.

In this work the optic fiber has to be coupled to the waveguide in order to send the light through the waveguide. In order to facilitate the easy coupling of the optic fiber to the waveguide, V grooves are formed in the silicon substrate. The V shaped grooves are anisotropically etched in the substrate.

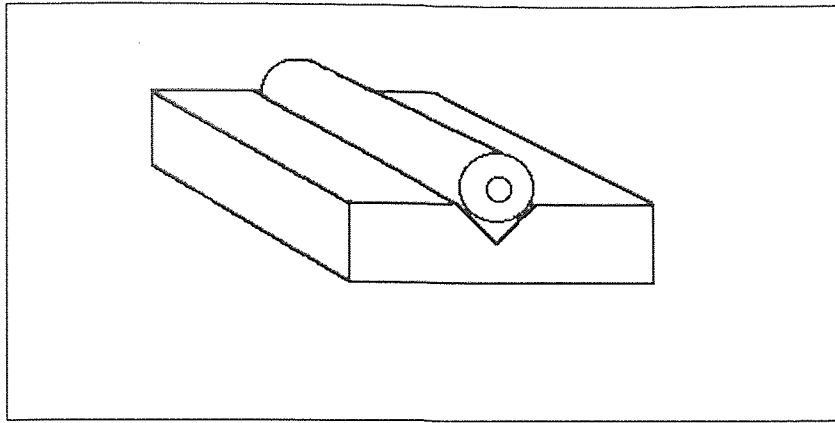


Figure 1.2 Optic fiber in a V groove etched anisotropically in silicon substrate

An array of parallel V grooves were defined (length = 4 mm, width = 150 μm , groove separation = 2 mm) in $\langle 100 \rangle$ silicon using photolithography. The masking layer was silicon nitride.

Silicon etches anisotropically in KOH. The etching proceeds in the (100) direction along the $\langle 111 \rangle$ plane. The etches self terminates. The figure 1.2 explains that. The V grooves etched in silicon have an intrinsic apex angle of $70^{\circ}31'44''$.

This work has focused on the synthesis of the materials required to fabricate the waveguide and the reference arm barrier and the fabrication of the sensor. Low pressure chemical vapor deposition (LPCVD) processes were developed to produce undoped and phosphorus-doped silicon dioxide films. The silicon nitride films were used as etch masks in the formation of the V-grooves in the silicon substrate where the optical fibers rest and couple to the planar waveguide structure. The undoped silicon dioxide was used as a thin glass buffer layer ($\sim 1 \mu\text{m}$) that protects the reference arm from the influence of pollutants and the thick layer ($\sim 10 \mu\text{m}$) that prevents the guided light from coupling with the

underlying Si substrate. The phosphorus doped (~8% P) silicon dioxide films are to be used as core material for the waveguide because of their higher refractive index (1.47) compared to the undoped oxide cladding (1.45). The silicon nitride films showed excellent etching resistance in KOH (used in the etching of Si V-grooves) were those synthesized using dichlorosilane (DCS) and ammonia at a temperature of 775°C, total pressure of 400 mTorr, and NH₃/DCS flow ratio of 2.4/1. The silicon nitride films were deposited using standard clean room technology. The undoped silicon dioxide films showing optimal refractive index characteristics were those synthesized using diethylsilane (DES) and oxygen at a temperature of 475°C, total pressure of 500 mTorr, and O₂/DES flow ratio of 1/2. Another technology developed for the growth of undoped oxide used DTBS and oxygen. Formation of the P doped oxide film was accomplished under the same processing conditions with the addition of a trimethylphosphite (TMP) precursor may be varied easily over a wide range (0-10%) with regulation of the TMP flow (0-8 sccm)

1.7 Lithography

1.7.1 Introduction

Fabrication of micro electro mechanical devices or optic devices on a silicon substrate requires working on a tiny region of the substrate. The patterns that define such regions are created by lithographic processes. That is layers of photoresist materials are first spin coated onto the wafer substrate. Next the resist layer is selectively exposed to a form of radiation, such as ultra violet light, electrons, or x rays. An exposure tool and mask, or a

data tape in electron beam lithography are used to effect the desired selective exposure. The patterns in the resist are formed when the wafer undergoes the subsequent “development” step. The areas of the resist remaining after development protect the substrate regions they cover. Locations from resist has been removed can be subjected to a variety of additive or subtractive processes that transfer the pattern onto the substrate surface.

1.7.2 Basic Photoresist Terminology

The basic steps of the lithographic process are shown in the figure. The photoresist (PR) is applied as a thin film to the substrate(e.g. SiO_2 on Si), and subsequently exposed through a mask. The mask contains clear and opaque features that define pattern to be created in the PR layer. The areas in the PR exposed to light are made either soluble or insoluble in a specific solvent known as developer. In the case when irradiated (exposed) regions are soluble, a positive image of the mask is produced in the resist. Such material is therefore termed a positive photoresist. On the other hand, if the non irradiated regions are dissolved by the developer, a negative image results. Hence the resist is termed a negative resist. Following development, the regions of SiO_2 no longer covered by resist, are removed by etching, thereby replicating the mask pattern in that oxide layer.

The resist is seen to perform two roles in this process. First, it must respond to exposing radiation in such a way that mask image can be replicated in the resist. Second, the remaining areas of resist must protect the underlying substrate during subsequent processing. In fact the name resist evolved from the ability to resist etchants.

Although both negative and positive resists are used to manufacture semiconductor components, the higher resolution capabilities of positive resists have virtually made them exclusive choice for VLSI applications. Conventional positive optical lithographic processes and resists are capable of producing images on VLSI substrates with dimensions as small as 0.8-1.5 μm . For submicron features, however, diffraction effects during exposure may ultimately cause other higher resolution techniques to replace optical lithography

1.8 Etching

1.8.1 Terminology of Etching

Etching in microelectronic fabrication is a process by which material is removed from the silicon substrate or from thin films on the substrate surface. When the mask layer is used to protect specific regions of the wafer surface, the goal of etching is to precisely remove the material which is not covered by the mask.

In general etching process is not completely attainable. That is etching process are not capable of transferring the pattern established by protective mask into the underlying material. Degree to which the process fail to to satisfy the ideal is specified by two parameters: bias and tolerance. *Bias* is the difference between the etched image and mask image. *Tolerance* is a measure of statistical distribution of bias values that characterizes the uniformity of etching.

The rate at which material is removed from the film by etching is known as etch rate. The units of *etch rate* are $\text{\AA}/\text{min}$, $\mu\text{m}/\text{min}$, etc. Generally high etch rates are

desirable as they allow higher production throughputs, but in some cases high etch rates make the control of lateral etching a problem. That is since material removal can occur in both horizontal and vertical directions, the horizontal etch rate as well as vertical etch rate may need to be established in order to characterize an etching process. The lateral etch ratio, L_R , is defined as the ratio of the etch rate in a horizontal direction to that in a vertical direction. Thus:

$$L_R = \frac{\text{Horizontal etch rate of material}}{\text{Vertical etch rate of material}}$$

In the case of an ideal etch process the mask pattern would be transferred to the underlying layer with a zero bias. This would then create a vertical edge of the mask. Therefore the lateral etch rate would also have to have been zero. For nonzero L_R , the film material is etched to some degree under the mask and this effect is called undercut. When the etching proceed in all directions at the same rate, it is said to be *isotropic*. The By definition, however, any etching that is not isotropic is anisotropic. If etching proceeds exclusively in one directions (e.g. only vertically), the etching process is said to be completely *anisotropic*. A typical anisotropic etch profile is shown in the figure 1.3

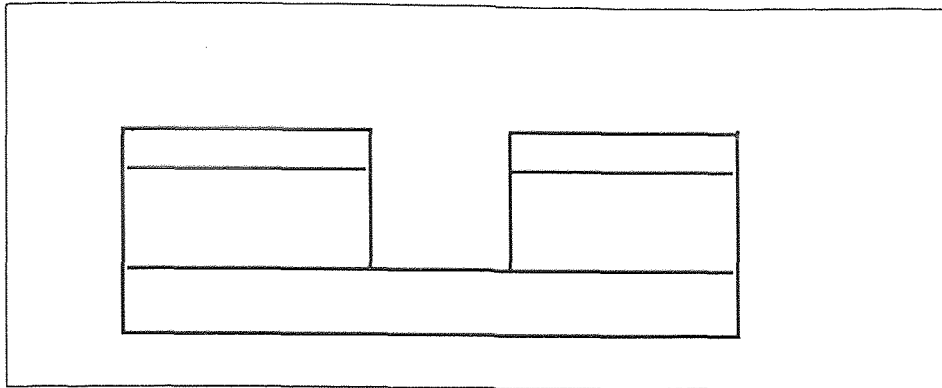


Figure 1.3 Anisotropic etch profile

So far it has been assumed that the mask is not attacked by the etchant and did not consider that the layers under the etched film can also be attacked by the etchant. In fact both the mask and the underlying layer materials are generally etchable, and these effects may play a significant role in specifying etch processes. The underlying material subject to attack may either be the silicon wafer itself, or a film grown or deposited during a previous fabrication step. The ratio of the etch rates of different materials is known as *selectivity of an etched process*. Thus both the selectivity with respect to the mask material and the selectivity with respect to the substrate materials are important characteristics of an etch process.

1.8.2 Wet Etching Technology

Wet etching processes are generally isotropic. They are inadequate for defining features less than $3\mu\text{m}$. Nevertheless for those processes that involve patterning of linewidths greater than $3\mu\text{m}$, wet etching continues to be a viable technology.

The reason wet etching has found widespread acceptance in microelectronic fabrication is that it is a low cost, reliable, high throughput process with excellent selectivity for most etch process with respect to both mask and substrate materials.

In general wet etch processes can be broken down into three steps:

- diffusion of the reactant to the reacting surface
- reaction
- diffusion of reaction products from the surface.

The second step can obviously be further differentiated into adsorption prior to, and desorption subsequent to, the actual reaction step. The slowest of the steps will be rate controlling. That is, the rate of that step will be the rate of the overall reaction.

Chemical etching can occur by several processes. The simplest involves dissolution of the material in a liquid solvent without any change in the chemical nature of the dissolved species. Most etching process, however, involve one or more chemical reactions. Various types of reactions may take place, although one commonly encountered in semiconductor fabrication is oxidation-reduction (redox). That is, a layer of oxide is formed, then the oxide is dissolved and the next layer of oxide is formed, etc (e.g. wet etching of Si and Al)

In semiconductor applications, wet etching is used to produce patterns on the silicon substrate or in thin films. A mask is typically used to protect desired surface regions from the etchant and this mask is stripped after the etching has been performed. Thus, when choosing a wet etch process, in addition to selecting an etchant, a suitable masking material must be picked to have good adhesion to the underlying films, good

coating integrity and ability to withstand attack by etchant. Photoresist is the most commonly encountered masking layer, but sometimes it falls short in this role. Problems involved include loss of adhesion at the edge of the mask-film interface due to etchant attack, and large area failure of the resist. Large area failures of the resist are usually due to differential stress buildups in the substrate and mask layers. Also bubble formation during etching process can lead to poor pattern definition, particularly at the pattern edges.

1.8.3 Dry Etching

Wet etching processes are typically isotropic, therefore if the thickness of the film being etched is comparable to the minimum pattern dimension, undercutting due to isotropic etching becomes intolerable. One alternative pattern transfer method that offers the capability of non isotropic(or anisotropic) etching is “dry etching”. As a result, considerable effort has been expended to develop dry etch processes as replacements for wet etch processes.

The overall goal of an etch process, as mentioned earlier, is to be able to reproduce the features on the mask with fidelity. This should be achievable together with control of following aspects of etched features:

- the slope of the feature sidewalls (e.g. the slope of the sidewalls of the etched feature should have the desired angle, in some cases vertical)
- the degree of undercutting(i.e. usually the less undercutting the better)

There are a variety of dry etch processes. The mechanism of etching in each type of process can have a physical bias(e.g. glow-discharge sputtering), a chemical bias(e.g. plasma etching), or a combination of the two(e.g. reactive ion etching, RIE, and reactive ion beam etching RIBE).

In processes that rely predominantly on the physical mechanism of sputtering (including RIBE), the strongly directional nature of the incident energetic ions allows substrate material to be removed in a highly anisotropic manner(i.e. essentially vertical etch profiles are produced). Unfortunately such material mechanisms are non selective against both masking material and materials underlying the layers being etched. That is, the selectivity depends largely on sputter yield differences between materials. On the other hand purely chemical mechanisms for etching can exhibit very high selectivities against both mask and underlying substrate material. Such purely chemical etching mechanisms, however, typically etch in an isotropic fashion.

By adding a physical component to a purely chemical etching mechanism, however the shortcomings of both sputter based and purely chemical dry etching process can be surmounted. Plasma etching process is a purely chemical process and reactive ion etching processes is a physical/chemical process.

The basic concept of plasma etching is rather direct. A glow discharge is utilized to produce chemically reactive species from a relatively inert molecular gas. The etching gas is chosen so as to generate species which react chemically with the material to be

etched, and whose reaction product is volatile. An ideal dry etch process based solely on chemical mechanisms for material removal, can thus be broken down into six steps:

- reactive species are generated in a plasma
- these species diffuse to the surface of the material being etched
- the species are adsorbed on the surface
- a chemical reaction occurs with the formation of a volatile by product
- the by product is desorbed from the surface
- the desorbed species diffuse into the bulk of the gas

If any of these steps fail to occur, the overall etch process ceases. Many reactive species can react rapidly with a solid surface, but unless the product has a reasonable vapor pressure so that desorption occurs, no etching takes place.

CHAPTER 2

REVIEW OF LITERATURE

2.1 Introduction

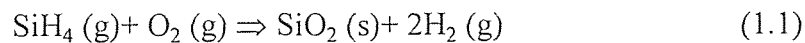
In this chapter a review of the various deposition techniques of silicon dioxide, Phosphosilicate glass, silicon nitride, and their properties will be discussed. A brief review of the various techniques to determine the phosphorus concentration in P-glass will also be discussed. A review is also made of the work done on Mach Zehnder interferometer and the various techniques to couple the optic fiber and the wave guide. Finally the aim and scope of this work will be discussed.

2.2 Deposition Techniques

SiO₂ film can be deposited by CVD in several ways, depending on the specific applications. The temperature ranges in which CVD SiO₂ film can be formed are:

- low temperature deposition, 300-450°C
- medium temperature deposition, 450-800°C
- high temperature deposition, above 800°C

In the lower temperature range, most of the early processes were based on silane chemistry:



The deposition can proceed in atmospheric pressure (APCVD) reactors [1-3], low pressure CVD (LPCVD) reactors [4-19], or plasma enhanced CVD (PECVD) [20-27].

APCVD employs a simpler and less expensive system, which is the main advantage over other ones that require vacuum environment. Because rates as large as 100 nm/min were readily attained [1,2], such reactors achieved very good throughput. Operation at atmospheric pressure, however, lends to the danger of gas phase nucleation which produced unacceptably high levels of defects, unless a high degree of inert gas diluent is used.

LPCVD produced cleaner films due to a reduction in gas phase nucleation. But the deposition rate based on the same chemistry (equation (1.1)) was found to be as low as 2-4 nm/min where the system throughput was not competitive though excellent uniformity of film thickness and composition were obtained [28].

2.2.1 LPCVD of SiO₂

LPCVD of silicon dioxide is generally based on the reaction of silane and oxygen. Various new precursors are now coming up in the place of silane not only for generating good quality films and optimizing the deposition conditions, but also for the safety purpose because silane is a toxic, pyrophoric and potentially explosive gas. Some of these precursors are listed in the table 2.1

Most of the work has been done with TEOS, using both LPCVD [13,29,38-41] and PECVD [20-25,30-33] techniques. Optimum deposition conditions and their effects on the deposit properties have been studied in detail.

Diethylsilane (DES), the precursor used in this study, has a vapor pressure as high as 200 mTorr at room temperature (25°C). It can be processed into the reactor without the need of a carrier gas. Heating of the liquid source and the delivery line is not necessary either. The main properties of DES are listed in table 2.2

Table 2.1 New precursors of CVD SiO₂

Name	Formula
Tetraethoxysilane (TEOS)	Si(OC ₂ H ₅) ₄
Ethyltriethoxysilane (ETOS)	C ₂ H ₅ Si(OC ₂ H ₅) ₃
Amyltriethoxysilane	C ₅ H ₁₁ Si(OC ₂ H ₅) ₃
Vinyltriethoxysilane	CH ₂ =CHSi(OC ₂ H ₅) ₃
Phenyldiethoxysilane	C ₆ H ₅ Si(OC ₂ H ₅) ₃
Dimethyldiethoxysilane	(CH ₃) ₂ Si(OC ₂ H ₅) ₂
Dipenyldiethoxysilane	(C ₆ H ₅) ₂ Si(OC ₂ H ₅) ₂
Tetrapropoxysilane	Si(OC ₃ H ₇) ₄
Tetrabutoxysilane	Si(OC ₄ H ₉) ₄
Diacetoxyditertiary- butoxysilane (DADBS)	(C ₂ H ₅ O) ₂ Si(OC ₃ H ₇) ₂
Diethylsilane (DES)	Si ₄ (CH ₃) ₈

Table 2.2 Properties of DES

Chemical Name	diethylsilane (DES)
Chemical formula	$\text{SiH}_2(\text{C}_2\text{H}_5)_2$
General Name	Organohydrosilane
Molecular weight	88.2
Appearance	colorless liquid
Solubility in water	Insoluble
Autoignition Temperature	218°C
Normal Boiling point	56°C
Flash point	-20°C (closed cup)
Freezing point	< -76°C (at 1 atm)
Density	0.6843 g/cm ³ @20°C
Vapor Density (air = 1)	>1
Vapor pressure	201 torr @20°C

2.2.2 Properties of Films Deposited Using DES

In their work, Levy et al, studied the film properties obtained by varying temperature, pressure, O₂ flow rate, O₂/DES ratio. They observed that the deposition rate decreases monotonically from 0.75 torr to 0.35 torr, where the deposition ceases abruptly. They evaluated the activation energy to be 10 Kcal/mol by studying the variation of deposition rate with temperature (in the range of 350-450°C).

The refractive index of the films were in the narrow range 1.453-1.456, independent of deposition conditions. The film stress was measured as a function of oxide film thickness for process conditions of 400°C, 5 Torr, 50 sccm DES and 100 sccm of O₂. The stress was found to be compressive and decreased with thickness. The density of the films were found to be 2.25g/cm³.

2.3 LPCVD of Phosphosilicate Glass

Low pressure chemical vapor deposition (LPCVD) of PSG films has generally been deposited using SiH₄:PH₃. Since PSG consists of two compounds, P₂O₅ and SiO₂, it is a binary glass, and some of its properties are considerably different from those of the undoped CVD SiO₂. For example APCVD PSG shows reduced stress and somewhat improved step coverage as compared to the undoped oxide.

It is relatively easy to incorporate the P₂O₅ into the PSG, as the SiH₄:PH₃ ratio in the gas flow controls the SiO₂:P₂O₅ ratio in the deposited film. PSG becomes increasingly hygroscopic at high P concentrations. Thus the P content should be maintained at 6-8 wt % to minimize phosphoric acid formation [41].

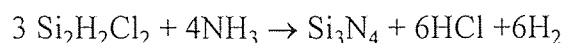
PSG has also been deposited using PECVD by the reaction of silane, N₂, O₂, PH₃ with Ar as the carrier gas.

Work has been done by Murarka and Adams [54] on measuring the P concentrations in PSG films. They compared the accuracy of measuring P concentration by each of the technique.

2.4 CVD of Silicon Nitride

Techniques used for depositing silicon nitride depends on its application. When it is used as a mask for selective oxidation or as a gate dielectric material in MNOS structures, it is deposited by high temperature LPCVD. When used as a passivation layer the deposition process must be compatible with such low melting materials like aluminum, thus PECVD is type method of choice [34-36].

LPCVD of silicon nitride is formed by reacting dichlorosilane and ammonia at temperatures between 700-800°C according to the overall reaction:



The Properties of PECVD silicon nitride and high temperature CVD nitride are listed in the table 2.3.

Table 2.3 Properties of Silicon nitride

Property	High temperature LPCVD	PECVD
Composition	Si_3N_4	$\text{Si}_x\text{N}_y\text{H}_z$
Density	2.8-3.1 g/cm ³	2.5-2.8 g/cm ³
Refractive index	2.0-2.1	2.1-2.1
Dielectric constant	6-7	6-9
Dielectric strength	10 ⁷	6x10 ⁶ V/cm
Bulk resistivity	10 ¹⁵ -10 ¹⁷	10 ¹⁵ ohms/cm
Step coverage	Fair	Conformal
Stress	1.2-1.8 x 10 ⁸ dyn/cm ² (tensile)	1-8x10 ⁹ dyn/cm ² (compressive)

Attempts have been made to obtain low stress silicon nitride [38-41]. Amorphous films were deposited at 300°C on single crystal Si and fused quartz substrates using SiH₄-NH₃ mixtures by PECVD technique. Increased tensile stress subsequent to a reduction in the compressive stress with increasing x was observed. It was found that the measured tensile stress in α -SiN _{x} :H films for high x above 1.0 was caused by the intrinsic stress, and that incorporated NH bonds act to act to relax the intrinsic stress.

The LPCVD silicon nitride has a very high tensile stress. Films rich in nitrogen are under tension. The stress increasing most rapidly as the composition near Si₃N₄.

2.5 Mach Zehnder Interferometer

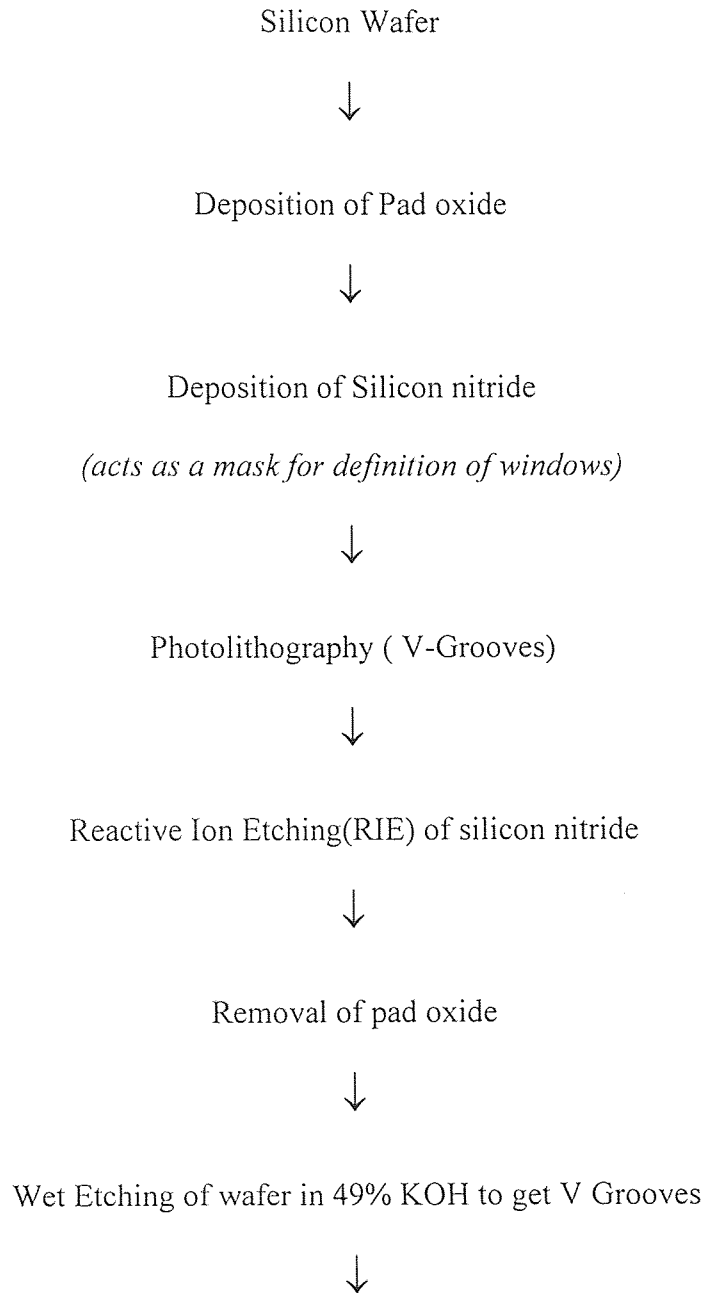
In the recent past, investigators have suggested optical techniques for remote monitoring of pollutants. These remote sensing devices use optical fibers or a combination of fiber coupling and a planar waveguide sensing device [42-45]. Several authors [46-49] report the use of planar waveguide interferometers as a basis for physical and chemical sensing. Lukosz calculated that an interferometric sensor could measure changes in refractive index that were approximately one order of magnitude smaller than the surface plasmon resonance approach. In majority of the cases, the above authors used planar waveguides. In most cases the substrate was SiO₂ on silicon. Boiarski et al [50] describe a channel waveguide device which integrates the splitting and combining portion of the interferometer on a glass substrate. The interferometric output was recorded as a function of arm length, for several liquids of known refractive index. Optical and physical

connection of optical fiber to the waveguide is an important step in the making of the device. There are several papers describing techniques to couple them [51-53]. Pigram et al describe fabrication of V-fiber interconnects and the integration of V fibers with devices. Yamada et al describe butt coupling technique. Rice et al describe self alignment technique to couple the fiber to the guided wave device.

CHAPTER 3

EXPERIMENTAL PROCEDURE

3.1 Flow sheet for fabrication of Mach Zehnder Interferometer



Removal of silicon nitride



Deposition of 10 μ m oxide

(to prevent light from being absorbed by the Si)



Deposition of P Glass(\sim 4 μ m)

(core layer of the waveguide)



Photolithography of P Glass

(to get the arms of the interferometer)



Reactive Ion Etching (RIE) of P Glass



Deposition of Oxide layer(\sim 2 μ m)

(cladding layer for the waveguide)



Photolithography of Oxide

(to form the cladding over the reference arm)



Reactive Ion Etching (RIE) of Oxide

3.2 Deposition of Thermal Oxide

3.2.1 Introduction

The formation of oxide of silicon on silicon surface is termed oxidation. The ability to form this oxide, which is stable and tenacious, provides the foundation for planar processing of silicon integrated circuits. Although there are several ways to produce SiO_2 directly on Si surface, it is most often accomplished by thermal oxidation, in which silicon is exposed to an oxidizing atmosphere (O_2 , H_2O) at elevated temperatures. Thermal oxidation is capable of producing SiO_2 with controlled thickness and Si/ SiO_2 interface properties.

Thermally grown SiO_2 is found in VLSI processing applications in thickness ranging from 60 Å to 10,000 Å. Some of the functions include:

- masking against ion implantation
- passivation of silicon surface
- isolation of individual devices
- use as a gate oxide and capacitor dielectric in MOS devices

The thermal oxide, in this case also referred to as a pad oxide (~250 Å) was deposited in the clean room, before the deposition of the silicon nitride. The pad oxide is supposed to reduce the stress on the substrate. This is so because thermally grown oxides are compressive in stresses and silicon nitride films are tensile in stress. The pad oxide also helps in reducing the pin holes during etching of silicon in the KOH in the further processing stages.

3.2.2 Deposition Procedure

The wafers are cleaned in the P-strip and P-clean solution respectively. The wafers are cleaned in each of them for 10 minutes. The wafers are then furnace pre-cleaned in a solution containing 100:1 H₂O-HF, to strip the wafer of the native oxide that may be present. They are then loaded into the reactor (the details of which are described in the next section) . The growth is carried out at a temperature of 950°C with an O₂ flow rate of 75 SLM. The deposition was done for 10 minutes.

3.3 Deposition of LPCVD Silicon Nitride

3.3.1 Introduction

Silicon nitride films have found wide applications in microelectronics. The most important application is its use as a mask during diffusion, surface passivation, gate insulation in semiconductor devices. Most often they are deposited using SiH₄-NH₃, SiCl₄-NH₃ or SiH₂Cl₂-NH₃. In this work silicon nitride films were deposited using the SiH₂Cl₂-NH₃. The films produced using this system at temperatures upto 800°C have amorphous structure. They are isotropic in properties and homogenous in composition, which is close to stoichiometric one.

The biggest problem with silicon nitride films is that they are under high tensile stresses. This opens the door for a host of problems and limitations in fabrication, device stability, and device failure. The most obvious ones are film cracking, especially at edges and contact windows, and bending of thin substrates by the induced strains. Slip in Si

crystal and the generation of dislocations are also likely to occur. This work has also involved attempts to produce low stress silicon nitride films.

Prior to the use of silicon nitride as a mask, Silicon carbide and boron nitride were tried as masks for etching of V grooves. The boron nitride was deposited using the following conditions.

Table 3.1 Conditions for deposition of Boron nitride

NH ₃ flow rate	500 sccm
TEAB flow rate	17 sccm
Temperature (°C)	550
Pressure (m Torr)	500
Time (min)	120

Table 3.2 The conditions for the deposition of silicon carbide

DTBS flow rate (sccm)	10
Temperature (°C)	550
Pressure (m Torr)	200
Time (min)	60

3.3.2 Description of LPCVD Reactor

The schematic of the LPCVD reactor is shown in the next section. The different steps involved in the deposition are also described there. The horizontal reaction chamber consists of 17.6 cm diameter fused quartz tube and 144 cm long encapsulated with a 3 zone, 10KW, Thermco MB-80 heating furnace. The flow of gases into the reaction chamber is controlled by MKS mass flow controllers. End caps designed for this reactor have a provision for cold water circulation to avoid overheating of the O rings. The temperature was kept a constant across all the zones and confirmed using a calibrated thermocouple. The entire deposition process was microprocessor controlled. The various steps of deposition are automatically performed till the end of deposition.

3.3.3 Deposition Procedure

Silicon nitride films were deposited on (100) oriented single crystals, single side polished Si wafers. The specifications of the wafer are tabulated in the next section. The silicon nitride that was to be used as a mask for the V-groove fabrication stage was deposited using the standard clean room conditions. Experiments were also performed to obtain low stress silicon nitride. The variations included changes in the flow rate of precursors, temperature of deposition, pressure. The deposition was carried out in most cases for a period of 50 minutes.

3.3.4 Experimental Details

The silicon nitride used as a mask for the lithographic process, was deposited using standard clean room process. The conditions are listed in the table

Table 3.3 Conditions for deposition of silicon nitride

NH ₃ flow rate (sccm)	120
DCS flow rate (sccm)	50
Temperature (°C)	775
Pressure (mTorr)	400

Experiments were also made to obtain low stress silicon nitride films. The experiments were made by altering the NH₃ flow rate, keeping the other parameters, i.e the DCS flow rate, temperature, pressure a constant. A run was also made altering the pressure, temperature and using an NH₃ flow of 10 sccm.

Stress analysis was conducted to determine the stress developed in the film on the silicon substrate based on an indigenously fabricated laser beam equipment. The details of this equipment are dealt with in the next section. The sample was also analyzed using Fourier transform infrared analysis technique.

3.4 Deposition of SiO₂ by LPCVD

3.4.1 Introduction

Low pressure chemical vapor deposition (LPCVD) of silicon dioxide is generally based on the reaction of SiH₄ and oxygen. The feasibility of using organic liquid sources like tetraethylorthosilicate (TEOS), ethyltriethoxysilane (ETOS), diacetoxydi-tert-butoxysilane (DADBS), to form silicon dioxide for microelectronic applications has been demonstrated by several researchers. Such liquid precursors offer numerous advantages over the use of silane including superior step coverage and increased safety.

DES is a precursor capable of producing oxide films at temperatures as low as 350^oC, thus allowing its use as a dielectric between aluminum metallization levels or as a top layer passivation coating. DES has several advantages over silane including superior conformality, low particulate formation, low stress, and high crack resistance. DES is a colorless liquid with a boiling point of 56^oC and freezing point less than -76^oC at atmospheric pressure. It exhibits a vapor pressure of 207 Torr at 20^oC.

Phosphosilicate glass or P-glass is deposited for use as the core of the waveguide. The P-glass is deposited using the same precursor as for oxide. The source for the Phosphorus being Trimethylphosphite (TMP). TMP does not have enough vapor pressure to flow into the chamber by itself. It is thus injected into the chamber.

3.4.2 LPCVD Reactor

The deposition reactor is schematically shown in Figure 3.1. This reactor was manufactured by Advanced Semiconductor Materials America Inc. (ASM America, Inc.) as a poly silicon micro-pressure CVD system. The horizontal reaction chamber consists of a 13.5 cm diameter fused quartz tube and a 144 cm long encapsulated with a three-zone, 10 K Watt, Thermco MB-80 heating furnace. The process tube door was constructed of a 300 series stainless steel, with a side hinge and sealed with an O-ring.

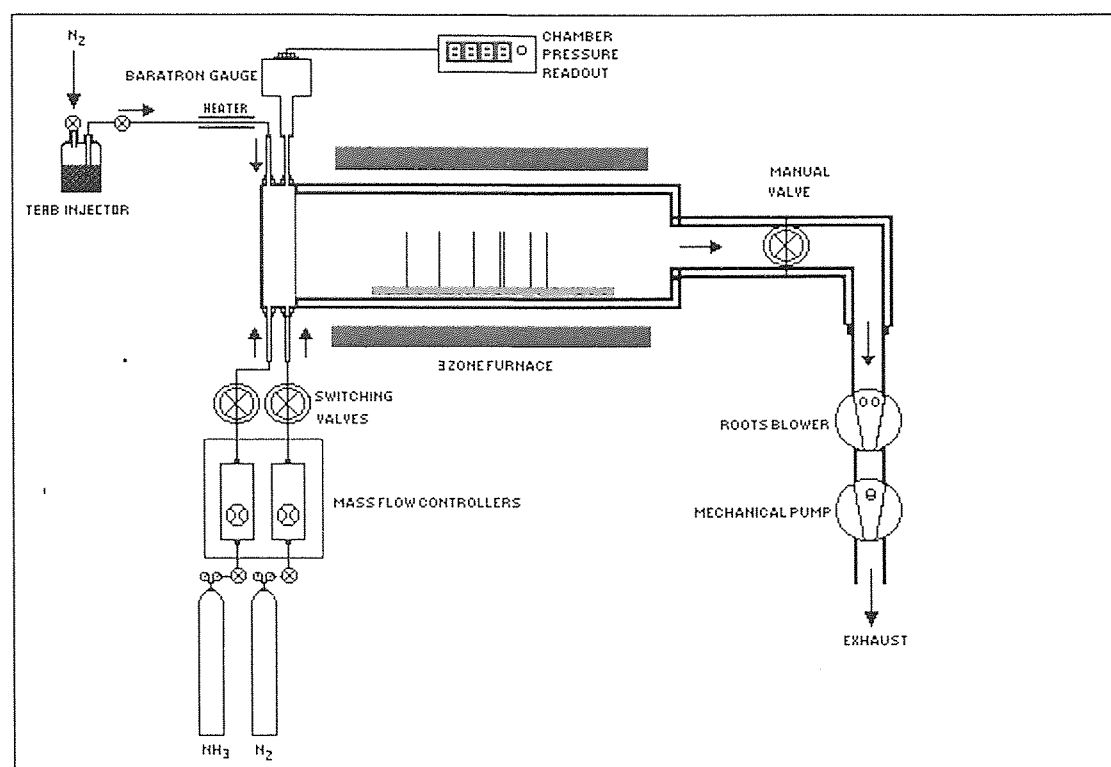


Figure 3.1 Schematic representation of the LPCVD reactor

The flow of oxygen into the reaction chamber is controlled by a MKS mass flow controller. A spare nitrogen mass flow controller was installed to incorporate any necessary additional reactant gas into the chamber or for backfilling. This spare controller could be calibrated for the gases other than nitrogen.

The other end of the reaction chamber is connected to a vacuum station comprised of a Leybold-Heraeus Trivac dual stage rotary vane pump backed by a Leybold-Heraeus roots pump to create the necessary vacuum in the system. An oil filter system is used to filter unnecessary particles from oil and thereby increasing the lifetime of the pump. End caps designed for this reactor have a provision for cold water circulation to avoid overheating of the O-rings. A ceramic tube was setup between the chamber and the heater to enhance the radiation heat transfer thus reducing the temperature deviation through the reaction tube. The temperature was kept constant across all zones and confirmed using a calibrated K type thermocouple. Mass flow controller set points were programmed with a MICON 3 microprocessing controller which produces the set point voltage and automatically monitors the flow vs. the programmed flow limits. The pressure in the reactor is monitored with an automatic exhaust valve and measured at the reactor inlet using a capacitance manometer (13 Torr MKS baratron pressure gauge).

3.4.3 Leakage Check

A leak would result in a change in the deposit structure (due to oxygen) and could result in haze depending on the size of the leak, therefore a leakage check in the CVD is an important step before making an experiment. When carrying out leak check, all

pneumatic controllers and gas regulators should be fully open to the gas cylinder main valves. The capillary is disconnected and the inlet is sealed with a plug because it is not possible to create vacuum in the capillary in the limited time period. After pumping the reaction system for a whole day, closing the outlet valve of the chamber, the pressure increasing rate was measured at a fixed period of time in the chamber to obtain the leakage rate. For this LPCVD system, the leakage rate deviated from 0.13 to 2 mTorr/min. Depending on the chamber condition a very low leak rate for a new chamber and higher leak rate for a chamber after long time in service. However, the leakage rate in the system was basically good.

3.4.4 Calibration of Gas Flow System

The flow rates for the reactant gas DES and O₂ were calibrated by noting the increase in pressure in the reaction chamber with increase in time (the vacuum outlet being sealed). Using the ideal gas law, $PV = nRT$, the following formula could be deduced to calibrate the flow rate.

$$\frac{dV}{dt} = \left(\frac{V_r}{760} \right) \left(\frac{273}{T_m} \right) \left(\frac{dP}{dt} \right)$$

dV/dt is the is the flow rate of the tested gas in sccm, V_r is the pre-calculated volume of the reactor ($20,900 \pm 600 \text{ cm}^3$), T_m is the measured chamber temperature in kelvin and dP/dt is the rate of pressure increase. The tested gas in the vacuum conditions considered as an ideal gas and the reaction chamber was evacuated for several hours before testing. After setting up the flow rate, the gas regulator was opened to introduce the gas flow into

the chamber, then the outlet valve of the chamber was closed and the pressure difference in the chamber was measured to obtain the rate of pressure increase. The real flow rate of the tested gas thus can be calculated using the above relation. The accuracy of this calibration involves the gas flow rate, the time interval, and the condition of the chamber should be carefully controlled. A smaller gas flow rate causes a slower pressure increase and thus leads to an easier detection of pressure increase and hence more accurate calibration. A longer time interval for calibration and a good vacuum condition in the chamber are also favored in the accuracy of calibration.

3.4.5 Liquid Injection System

The liquid injection system, designed and fabricated in house, consists of a glass bubbler connected to a precalibrated capillary tube fastened onto the reaction chamber. The flow rate is inversely proportional to the length of the capillary, while proportional to the pressure differential and the cross sectional area. The injection system has filters for both nitrogen purge and liquid precursor. The bubbler is always maintained at a positive pressure to prevent oxygen leak into it.

The liquid injection mechanism is used to inject TMP, the source of P, in the deposition of P-glass. In this case the injection mechanism is used for the lack of a flow controller for flowing the vapor.

3.5 Deposition Procedure

Silicondioxide films were deposited on (100) oriented single crystal, single-side polished Si wafers (obtained from Silicon Sense Inc.), and fused quartz wafers (obtained from Hoya, Japan). The details of the Si wafers is given in table.

The wafers are labeled and accurately weighed (up to 4 decimal places) using an electronic balance. These wafers are then placed on a quartz boat. The wafers used to measure the stress on the film are placed back-to-back at a distance of 65 cm from the reactor opening and the quartz wafer at a distance of 15 cm from the stress monitors in all the experiments.

Table 3.4 Specifications of the Si wafer

Source	Silicon Sense Inc.
Diameter	100 mm
Orientation	<100>
Thickness	$525 \pm 25 \mu\text{m}$
Type/Dopant	p/Boron
	n/Phosphorus
Resistivity	5 - 15 $\Omega\text{-cm}$
Grade	Test

A low pressure is maintained inside the chamber using the vacuum pumps. DES is flowed into the reaction chamber. The time of deposition was two hours in all the runs. Among the deposition parameters recorded were the background pressure, reaction temperature, flow rates of the reactants.

Samples are allowed to cool to room temperature and the wafers are removed from the reactor by introducing nitrogen to fill the vacuum chamber and rise the pressure to atmospheric pressure. The samples are then weighed and the deposition rate can be calculated by knowing the mass gain (mg/hr) due to deposition. Samples were observed in an optical microscope for the presence of microcracks and for gas phase nucleation.

3.5.1 Experimental Details

Table 3.5 The silicon dioxide films were deposited with the following conditions

DES flow rate (sccm)	30
O ₂ flow rate (sccm)	17
Temperature (°C)	475
Pressure (mTorr)	500

The runs were all made for 2 hours to test for the consistency of results. Once consistent results were obtained, long runs were made to obtain thick films (~10 μ m), the purpose of this experiment. The runs were made for 6 hours at a stretch. A couple of runs were made

with variations in flow rate of O₂ to obtain desired properties. P-glass was also deposited under same conditions, the source of P being Trimethylphosphite (TMP).

Fourier transform infrared (FTIR) spectra of the films obtained from Perkin - Elmer 580 were observed for Si-O peaks, SiOH peaks, water peaks and P=O peaks in the case of P-glass. Stress analysis was conducted to determine the stress developed in the film on the silicon substrate based on an indigenously fabricated laser beam equipment. The principle being the change in the radius of curvature of the film before and after deposition. Stress is calculated using Stony's formula

$$\sigma_s = ED^2/6(1-\nu)Rt$$

where E and ν are Young's modulus and Poisson ratio of the substrate. D, t are the substrate and film thickness' respectively, R is the radius of curvature of the composite. By convention R is negative for a complex wafer surface (compressive film stress) and positive for a concave wafer surface (tensile film stress). In the present set of experiments for the wafers used and considering the geometry of the instrument used, the equation reduces to

$$\sigma_s(\text{MPa}) = 12.3R'/t (\mu\text{m})$$

where R' is the difference of the deflection of the projected laser spots after and before deposition.

Refractive index of the silicon dioxide films was determined using Rudolph Research/Autodec ellipsometry. The measurement technique is mainly concerned with the measurement of changes and the state of polarization of light upon reflection with the surface. It employs monochromatic, plane polarized light with its plane of polarization

45° to the plane of incidence. When the elliptically polarized light is reflected from an absorbing substrate its state of polarization is changed. The ellipticity of the reflected beam is determined by the relative phase difference δ and azimuth ψ . An in-built computer program numerically solves the equations generated by these δ and ψ and the refractive index and the thickness of the film is obtained. In all the experiments the angle of incidence was maintained at 70° and the wavelength at 5461Å. Readings were taken at 5 places on the wafer and was averaged out.

The thickness of the films were measured using Nanometrics Nanospec/AFT nanospectrometer. The average refractive index obtained from the ellipsometer for that particular wafer was fed in and the thickness was measured in 5 places and averaged out.

In the case of P-glass, the samples are analyzed in the same way as the oxide wafers. The Phosphorus content in the films can be found by many techniques, including direct chemical analysis, neutron activation analysis, infrared absorption, electron microprobe, etch rate variation, sheet resistivity after a standard diffusion and variation in the refractive index of the films. In this work the variation in the refractive index and the etch rate variation techniques have been utilized to determine the P content in the films.

In the refractive index technique, the refractive index of the samples is found at various positions on the wafer and the refractive index is averaged out. This technique is described by others. The P content of the given sample is found by comparing it with the calibration plot of refractive index vs P content.

In the etch rate variation technique, the samples are etched at 25°C using P-etch solution (2 parts 70% HNO₃, 3 parts 49% HF, 60 parts H₂O). The etch rates are

determined by plotting film thickness vs the etch time. The etch rate calibration curve, i.e a plot of etch rate Vs P content will give the P content for the given sample.

3.6 Photolithography

3.6.1 Introduction

The first chapter has already dealt with the basics of lithography, the basic terminology involved in lithographic processes.

3.6.2 Description of Lithographic Process

The first step in this process is the application of photoresist. The photoresist is applied by spin coating technique. This procedure involves three stages : a)dispensing the resist solution onto the wafer; b) accelerating the wafer to the final rotational speed; and c) spinning at a constant speed to establish the desired thickness (and to dry the film).

The dispensing stage can either be accomplished by flooding the entire wafer with resist solution before the beginning the spinning, or by dispensing a smaller volume of resist solution at the center of the wafer and spinning at lower speeds to produce a uniform liquid layer across the wafer.

In the next stage the wafers are normally accelerated as quickly as is practical to the final spin speed and finally spinning at the constant speed to obtain desired thickness.

In this work the rotational speed was maintained at 1500 rpm. The wafers were spun at this speed for a period of 20 seconds. This gave a photoresist of 2 μ m thickness. Prior to exposure the wafers are baked for one minute at 115 $^{\circ}$ C or for a period of 20

minutes in an air oven maintained at the same temperature in order to remove the moisture present. The baking is done to remove the moisture from the wafer. Moisture can reduce the adhesion.

The exposure was carried out using a SUSS MA6 mask aligner. The lamphouse is equipped with a 350 W mercury high pressure lamp and a SUSS diffraction reducing optics. The usable wavelength falls between 350-450 nm. The lamphouse has an ellipsoidal mirror, and a 45° cold light mirror. The type of exposure lamp depends on the optical range selected. The cold light mirror reflects the desired short wavelength UV light through a fly's lens and transmits the longer wavelengths to a heat sink located in the bottom of the lamphouse. The lamphouse also contains a condenser lens, diffraction reducing lens plates, a 45° turning mirror and a collimation lens. A holder is provided in the mirror house for a filter. SUSS diffraction reducing exposure system provides a high resolution over the entire exposure area, resulting in steep resist edges and small diffraction effects.

The wafers were exposed for 20 seconds in the SUSS MA6 mask aligner. After the exposure the wafer must undergo "development" in order to leave behind the image which will serve as a mask for etching. The developer is poured on the wafer and allowed to develop for 30 second before it is spun at a high rpm(~2000-3000). This procedure is repeated for another 10 seconds of development. The wafer is then washed with DI water and spun again to remove all the water. The wafers are baked as before to rid of the moisture that may be absorbed by the substrate. The windows are then inspected under the microscope for their integrity.

3.7 Reactive Ion Etching

3.7.1 Introduction

Reactive ion etching as described before is an anisotropic etching technique. After the lithographic step, windows are formed on the photoresist layer. The silicon nitride is exposed in these windows. RIE is carried out to remove this silicon nitride and expose the underlying silicon substrate.

3.7.2 Description of the Reactor for RIE

Plasma etching systems consist of several components: a) an etching chamber, that is evacuated to reduced pressures; b) a pumping system for establishing and maintaining the reduced pressure; c) pressure gauges to monitor the pressure in the chamber; d) a variable conductance between the pump and etching chamber so that the pressure and flow rate in the chamber can be controlled independently; e) an RF power supply to create the glow discharge; f) a gas handling capability to meter and control the flow of reactant gases; and g) electrodes. There are several types of commercially available etching systems. They include :

1. barrel reactors
2. “downstream” etchers
3. parallel-electrode(planar) reactor etchers
4. stacked parallel-electrode etchers
5. hexode batch etchers

6. magnetron ion etchers

The RIE system in the class 10 clean room, where the fabrication of the V grooves was carried out, is a stacked parallel electrode etching system.

The stacked parallel electrode etcher is a small batch machine capable of handling 6 wafers at a time. Its unique design provides an individual pair of electrodes for each wafer thereby combining some of the advantages of a single wafer and batch etchers. Operating chamber pressures and rf power densities can be kept in the ranges between those of low pressure, low power density hexode batch etchers, and high pressure, high power density single wafer RIE machines.

3.7.3 Description of RIE Process

The silicon nitride was etched using standard clean room conditions. They are given in the table

Table 3.6 Conditions for etching of Silicon nitride

Power	400 W
Pressure	150 mTorr
Flow rate of SF ₆	50 sccm
Temperature	25°C

The etch rate for silicon nitride is 388 Å/min under these conditions. Thus the etch time is decided depending on the thickness of the nitride.

$$\text{Etch Time (min)} = \frac{\text{Thickness of the silicon nitride}(\text{\AA})}{\text{Etch Rate}(\text{\AA}/\text{min})}$$

The third slot from the top, in the etch reactor, was found to have a good etch uniformity. The wafers were etched one at a time in this slot. Care was taken during the removal of the wafer to prevent scratching of the wafer. The scratch can lead to pin holes during the KOH etching stage. The wafers were observed under the microscope for the completion of etching.

The photoresist is then stripped off using P-strip solution (5:1 H₂SO₄-H₂O₂). The wafers were dipped in a bath containing the P-strip solution, maintained at 110 °C, for 10 minutes. Then the wafers are washed for 10 minutes in deionised water (DI) and then for 5 minutes in cold DI water. The wafers are then dried in a spin dryer.

Prior to the use of silicon nitride as a mask, as mentioned before the silicon carbide and boron nitride were used as masks. Dry etch studies were carried out on these films using a parallel plate plasma etching system. The conditions for etching were the following:

Table 3.7 Conditions for etching of SiO₂

Power	200 W
Pressure	300 mTorr
Flow rate of CF ₄	50 sccm
Temperature	25°C

3.8 Etching of Wafers in 49% KOH

The windows, after etching the silicon nitride still have a pad oxide on it. Thus the pad oxide has to be removed before they are immersed in KOH. The pad oxide stripping is done in the 100:1 H₂O-HF solution. The etch time is calculated based on the etch rate of the pad oxide and its thickness. The wafers are then immersed in the bath containing 49% KOH maintained at 80°C for the time required for self termination of V grooves. The depth of the V grooves are measured using a micrometer in the optical microscope by focusing on the top and the bottom of the groove.

3.9 Stripping of Silicon Nitride

After the formation of the V grooves, the silicon nitride has served its purpose as a mask. It can thus be stripped off. The stripping of silicon nitride is done in hot phosphoric acid.

The bath is maintained at 170°C. The etch time depends on the thickness of the silicon nitride layer and the etch rate of silicon nitride in the bath at those conditions.

CHAPTER 4

RESULTS AND DISCUSSION

4.1 Introduction

The results of the experiments detailed in the previous chapter are described in this chapter. The results will be discussed in different sections in the order of the steps involved in the fabrication of the Mach Zehnder interferometer.

4.2 LPCVD of Silicon Nitride

Silicon nitride films deposited were very uniform. The growth rate for deposition was 50 Å/min. The stress for these films were very high (~700 MPa). They were tensile in nature and thus prone to cracking very easily. Thus the films were not grown to very large thickness. The deposition was carried out for 50 minutes. The silicon nitride was very resistant to KOH during the V groove etching stage. There was minimal pin hole formation. The few that were formed, were in the wafer periphery and not on the wafer surface, thus not affecting the device.

The attempts to obtain low stress silicon nitride was a failure. The flow of NH_3 was reduced in order to make the films silicon rich and thus less tensile. The temperature, pressure and DCS flow rate were maintained a constant.

From the figure 4.1, it can be seen that the stress values are almost independent of the flow rate for the given temperature, pressure and flow rate of DCS. The high NH_3 flow experiment for completeness of the study.

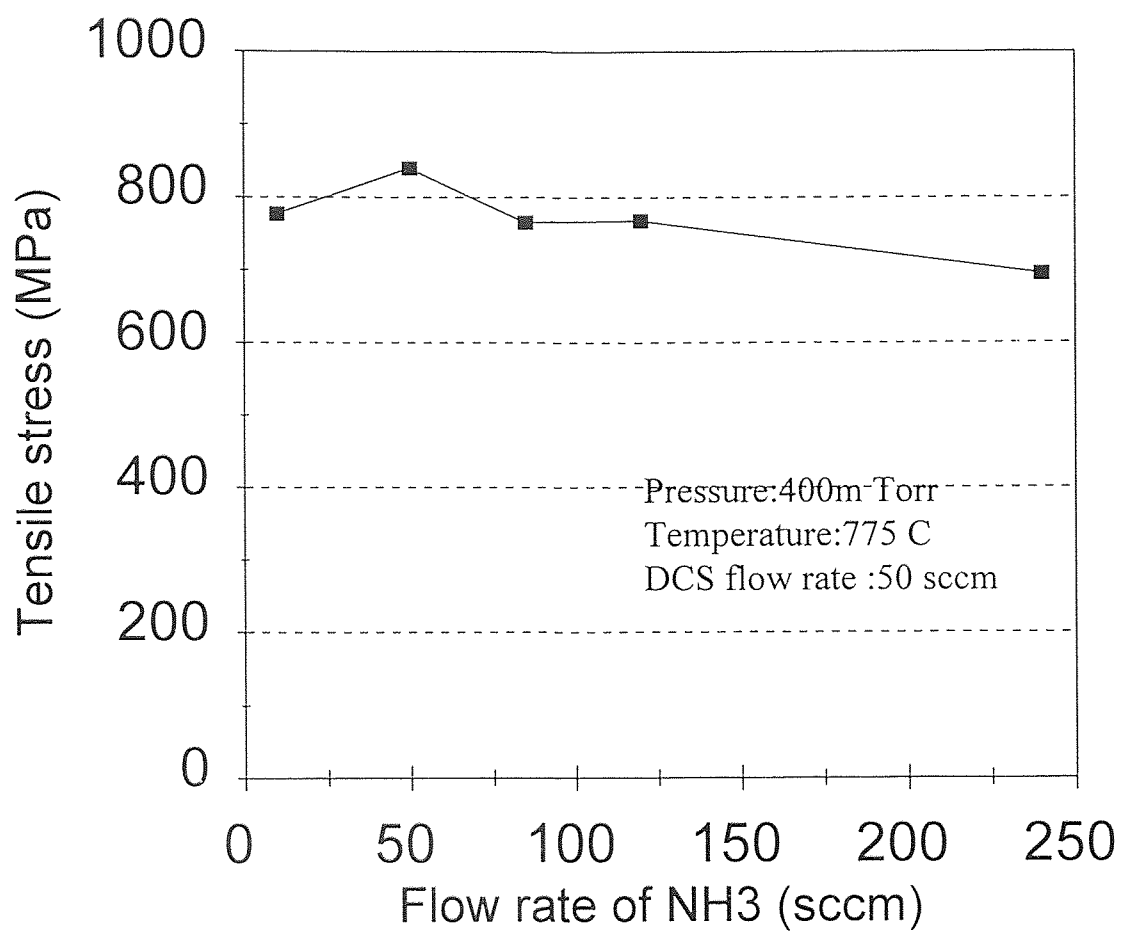


Figure 4.1 Plot of stress Vs flow rate of NH_3

The experiments were carried out both on virgin silicon wafers and wafers with a pad oxide ($\sim 250 \text{ \AA}$) on them. The stress values obtained in both cases yielded the same result. Thus the pad oxide does not play a role in reducing the stress in the film.

4.2.1 RIE of Silicon Nitride

The etch rate of silicon nitride was $388 \text{ \AA}/\text{min}$. Thus the film was etched for 6-7 minutes (film thickness was approximately 2500 \AA). The etching was very uniform. Once the silicon nitride was entirely removed, the wafers were stripped off their pad oxide (in the windows) in the 100:1 H_2O -HF.

4.3 LPCVD of SiO_2 and Phosphosilicate-glass

This section deals with the results obtained during the LPCVD experiments to deposit SiO_2 and Phosphosilicate glass.

4.3.1 FTIR Analysis of SiO_2

The figure shows the FTIR spectrum of SiO_2 in the range of 4000 cm^{-1} to 400 cm^{-1} for the oxide deposited at 475°C . The figure shows the Si-O peaks at 1060 , 800 and 440 cm^{-1} corresponding to stretching, bending, and rocking modes respectively.

The growth rate for the oxide is $130 \text{ \AA}/\text{min}$. The depositions were carried out for a period of 2 hours. The thickness of the film was very uniform over the entire wafer. There was a large depletion ($\sim 2000 \text{ \AA}$) observed between the first and the second wafer

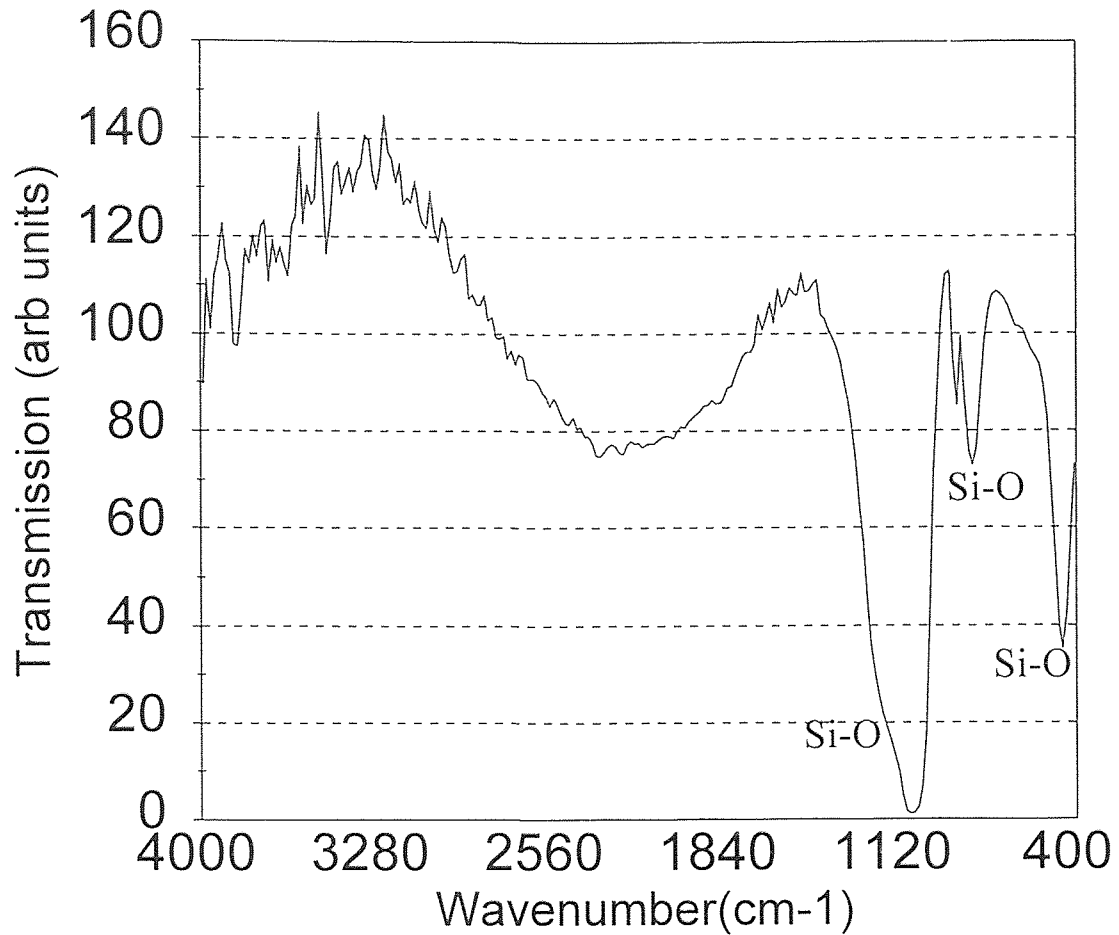


Figure 4.2 FTIR spectrum of silicon dioxide deposited at 475°C

The two most important parameters required of the film for use in Mach Zehnder interferometer is the stress and the refractive index. The stress was found to be 188 MPa and it was tensile in nature. The refractive index was 1.453 for the films. The UV spectroscopy showed the films to be transparent to the extent of 97%.

In the 6 hour run made to deposit a thick oxide, the wafers showed signs of cracking and the stress values were also low, indicating possible stress release upon cracking. Thus this technology though yielded good properties in terms of the refractive index and transparency of films, was not good for depositing thick layers.

Thus another technology was developed for the deposition of thick oxide. This process used Ditertiarybutylsilane (DTBS) and oxygen as precursors. The deposition was carried at a temperature of 700°C and a pressure of 200 mTorr. The growth rate of the films was about 100 Å/min. The stress was 5 MPa and was compressive in nature. Thus thick films could be deposited very easily. The refractive index was found to be 1.45.

4.3.2 FTIR analysis of P-glass

The figure shows the FTIR spectrum of P-glass with the characteristic P=O peak at 1323 cm^{-1} , in addition to the Si-O peaks observed at 1060, 800 and 440 cm^{-1} .

The growth rate of the P-glass was found to be 210Å/min. The films were fairly uniform over the entire wafer surface. There wasn't as much depletion observed in this case as compared to the oxide wafers. The stress in the film was 90 MPa and tensile in nature. Thus it can be seen that there is a two fold decrease in the stress with the presence of Phosphorus. The refractive index of the films ranged between 1.47-1.48. This difference in the refractive indices of the undoped oxide and P-glass was ideally suited for fabrication of waveguides.

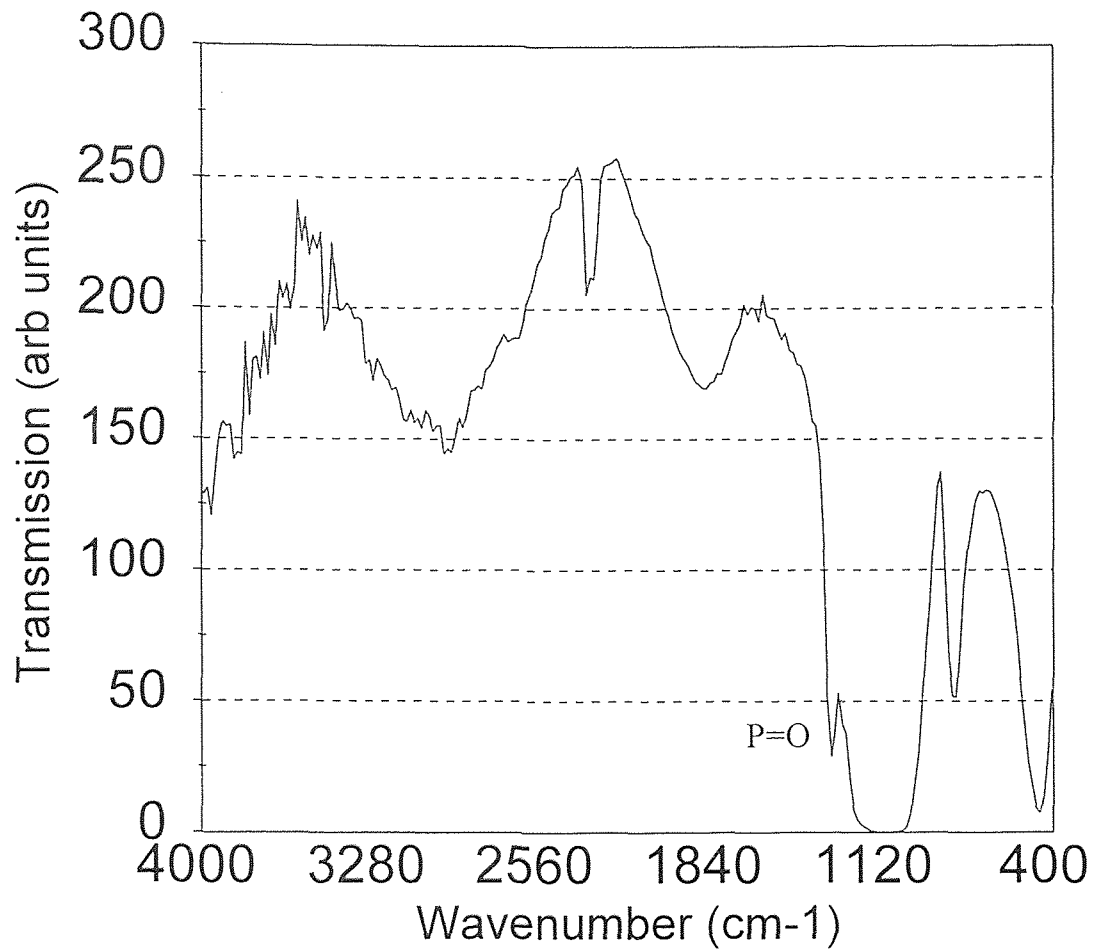


Figure 4.3 FTIR spectrum of Phosphosilicate glass

This technology though successful in depositing 3-4 μ m thick film required for the purpose, still had a high stress value. The new technology developed for the undoped oxide was also used to deposit P-glass films. The refractive index was in the range of 1.48-1.49

4.3.2.1: Determination of Phosphorus content: As mentioned before the refractive index and the etch rate of P glass in the P-etch solution were used to measure the P content. From the refractive index values, the P content was found to be in the range of 8-10%.

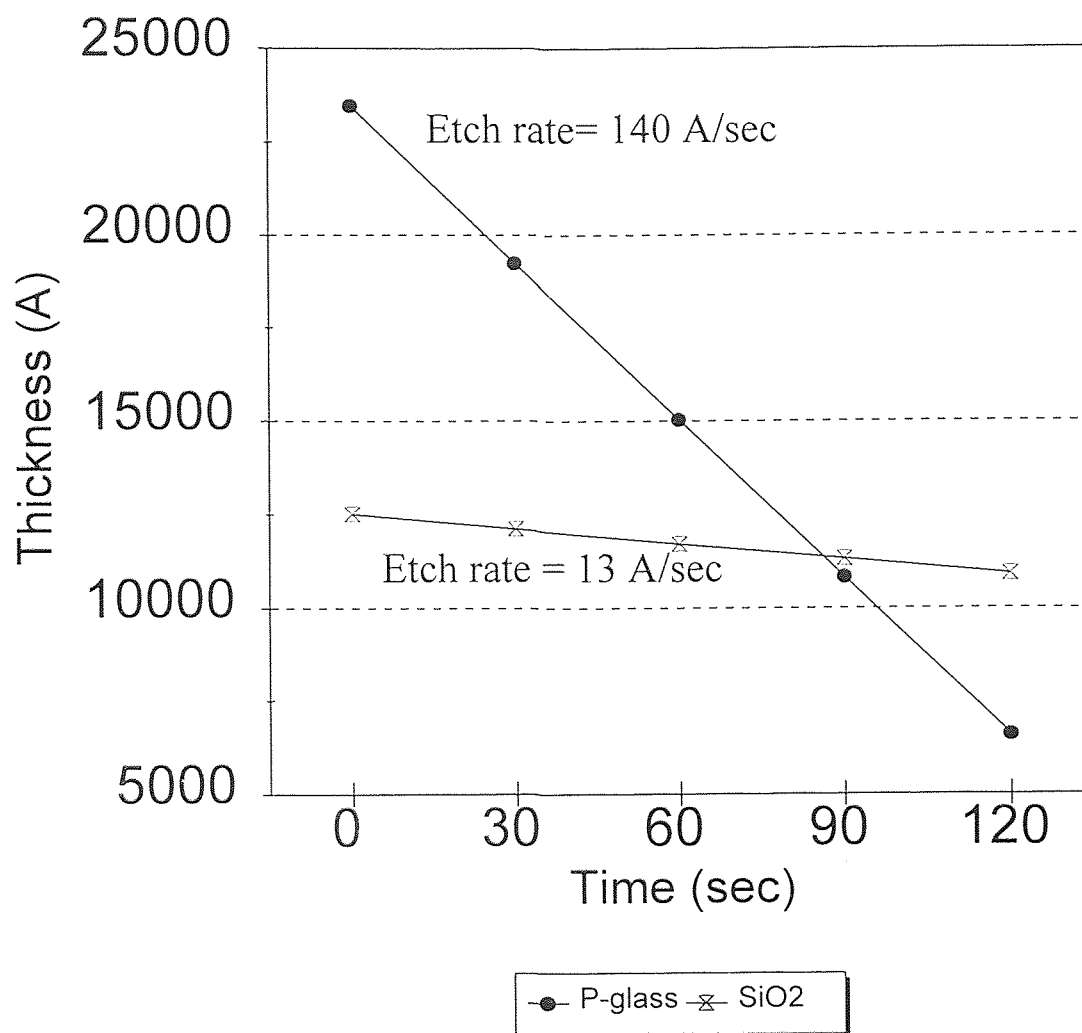


Figure 4.4 Etch rates of silicondioxide and P-glass in P-etch solution

The figure 4.4 shows the thickness V_s etch time. The slope of the curve gives the etch rate. The etch rate of P-glass in the P etch solution was $140 \text{ \AA}/\text{sec}$. This corresponded to a P content of 9-10% on the calibration curve. The undoped oxide showed a greater resistance.

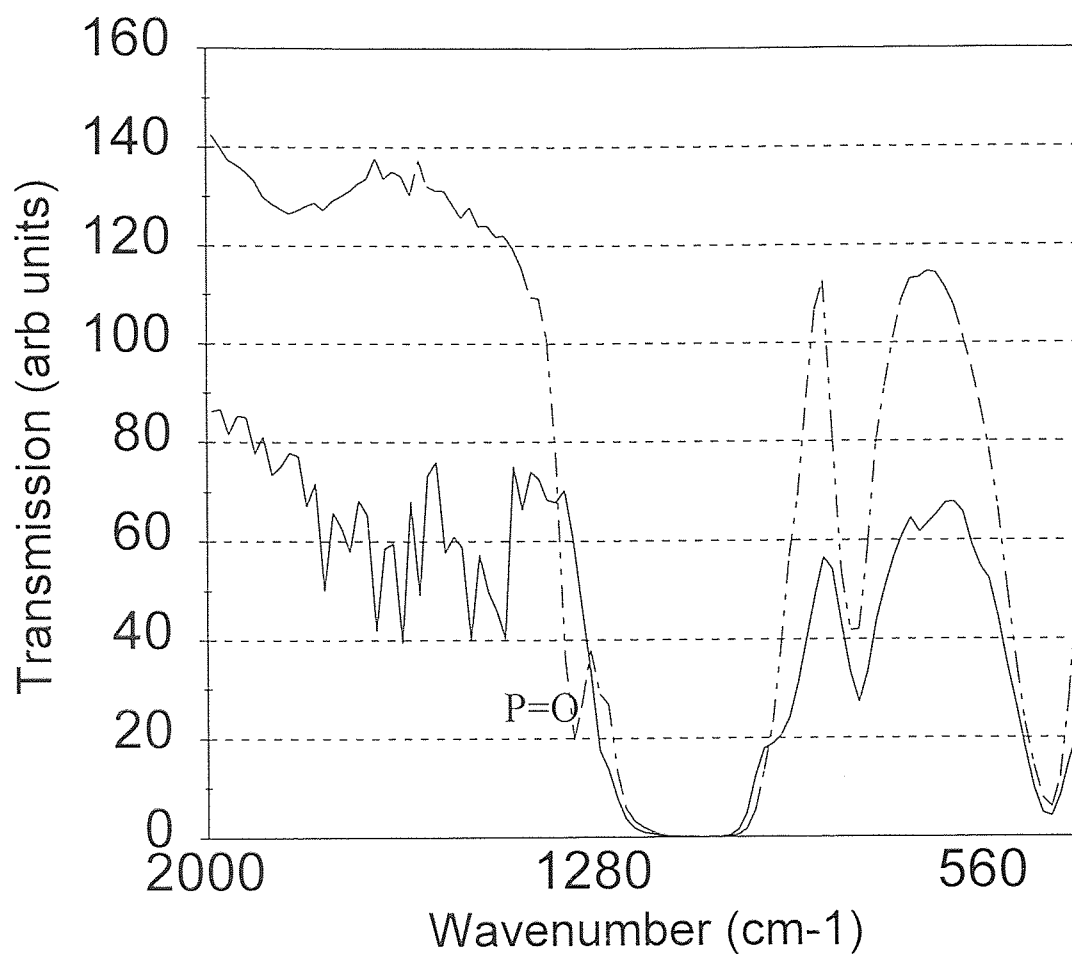


Figure 4.5 Comparison of P=O peaks after the film is exposed to atmosphere for 5 months

A high P concentration (~8-10%) will make the film hygroscopic, i.e. the film will start absorbing moisture from the atmosphere. There is formation of phosphoric acid. Figure 4.5 shows the comparison of the FTIR spectra of a P glass sample (~9%) immediately after deposition and after 5 months of exposure to atmospheric conditions. The dotted line is the spectrum of the sample soon after deposition. It can be seen that the Phosphorus peak has almost vanished after exposure to atmosphere.

4.4 Wet Etching of Wafers in KOH (to fabricate V grooves)

The <100> silicon wafers etch anisotropically in KOH. The etch rate in the (100) direction ranged from 0.75-1.0 $\mu\text{m}/\text{min}$. The wafers were etched for 3 hours to ensure self termination of the V grooves. On the other hand, the wafers were not etched for too long a time as pin hole formation could increase.

The depth of the V grooves was measured using an optical microscope. In most of the cases the self termination was achieved.

Prior to the use of the silicon nitride as a mask, silicon carbide and boron nitride were used. The processing was done under laboratory conditions. Thus the V grooves were not formed properly.

CHAPTER 5

CONCLUSIONS

This thesis has mainly focussed on the synthesis of materials required to fabricate the waveguide and in the fabrication of V grooves in the silicon substrate to facilitate easy coupling of the optic fiber to the waveguide. LPCVD processes were developed for undoped and doped silicon di oxide using DES as the precursor. The films obtained were uniform and had refractive index values required of them. The stress values were high and they were tensile in nature. Due to problems of film cracking, thick films could not be deposited. Alternate technology was developed by other workers to produce undoped and doped silicon dioxide [53,54].

An attempt was made to use boron nitride and silicon carbide as etch masks for the fabrication of V grooves. The V grooves showed pin holes. The V groove fabrication was done outside the clean room. Silicon Nitride was successfully used to serve as an etch mask. The deposition was carried out in the clean room and the entire fabrication sequence for the V grooves was also carried out in the clean room. The V grooves obtained were of good quality and had minimal pin holes. Dry etch processes were developed to etch undoped SiO_2 and doped SiO_2 .

Further work that has been going on towards the completion of this thesis has not been reported. Aluminum is being used as a mask for the etching doped SiO_2 due to improper selectivity obtained between the photoresist and the doped oxide for the given

etch process for the etching of SiO_2 is also being developed. Condition for the flowing of the P doped oxide, the core of the waveguides, is also being optimised.

REFERENCES

1. N. Goldsmith, W. Kern, *RCA Rev.*, 1967, 28, 153
2. C. Cobianu, C. Pavelescu, *J. Electrochem. Soc.*, 1983, 130, 1888
3. C. Cobianu, C. Pavelescu, *Thin Solid Films*, 1984, 117, 211
4. F.S. Becker, D. Pawlick, H. Schafr, G. Standigl, *J. Vac. Sci. Technol.*, 1986, B4(3), 732
5. H. Huppertz, W.L. Engl, *IEEE Trans. Electron Devices*, 1979, ED-26, 658
6. A.K. Hochberg, A. Lagendijk, D.L. O'Meara, J.J. Klerer, *J. Electrochem. Soc.*, 1961, 108, 1070,
7. E.L. Jordan, *ibid.*, 1961, 108, 478
8. J. Klereer, *ibid.*, 1965, 112 (5), 503
9. A.K. Hochberg, D.L. O'Meara, *ibid.*, 1989, 136 (6), 1843
10. J. Orshonik, J. Kraitchman, *ibid.*, 1968, 115, 649
11. R.A. Levy, P.K. Gallagher, F. Schrey, *ibid.*, 1987, 134, 430, 1744
12. J.M. Albella, A. Criado, E. Muroz Merino, *Thin Solid Films*, 1976, 36, 479
13. R.A. Levy, J.M. Grow, G.S. Chakravarthy, *Chem. Mater.*, 1993, 5, 1710
14. D.T.C. Huo, M.F. Yan, P.D. Foo, *J. Vac. Sci. Technol.*, 1991, A9, (5), 2602
15. J.D. Patterson, M.C. Ozturk, *ibid.*, 1992, B10(2), 625
16. B. Gelertt, *Semicond. Int.*, 1990, 13, 83
17. A.K. Hochberg, A. Lagendijk, D.L. O'Meara, *J. Electrochem. Soc.*, Ext. Abstr., 1988, 88-2, 335
18. A.C. Adams, C.D. Capio, *J. Electrochem. Soc.*, 1979, 126, 1042
19. A.C. Adams, F.B. Alexander, Capio, T.E. Smith, *ibid.*, 1981, 128, 1545

20. T. Emesh, G. D'Asti, J.S. Mercier, P. Leung, *ibid.*, 1989, 136, 3404
21. F. Fracassi, R. D'Agostino, P. Favio, *ibid.*, 1992, 139, 2636
22. P.G.T. Evert, Van de Ven, *Solid State Technol.*, 1981, 24 (4), 167
23. U. Mackens, U. Merkt, *Thin Solid Films*, 1982, 97, 53
24. B.L. Chin, P.G.T. Evert, Van de Ven, *Solid State Technol.*, 1988, 31 (4), 119
25. C.S. Gorthy, "Low Temperature Synthesis and Characterization of LPCVD Silicon di oxide using Di ethyl silane", MS. Thesis, Dept. of Matl. Sci. & Engg., New Jersey Institute of Technology, Newark, New Jersey, 1992
26. A. Datta, "Synthesis of silicon di oxide/vycor composite membrane structures by an optimized LPCVD process", MS thesis, Dept. of Matl. Sci. & Engg., New Jersey Institute of Technology, Newark, New Jersey, 1992
27. J.M. Grow, R.A. Levy, Y. Yu, K.T. Shih, *Mat. Res. Symp. Proc.*, 1994, 344, 241
28. R.S. Rosler, *Solid State Technol.*, 1977, 20 (4), 63
29. W.A. Brown, T.I. Kamins, *Solid State Technol.*, 1979, 22 (7), 51
30. F. Fracassi, R. d'Agostino, P. Favia, *ibid.*, 1992, 139 (9), 2636
31. C.S. Pai, C.P. Chang, *J. Appl. Phys.*, 1990, 68, 793
32. C.P. Chang, C.S. Pai, J.J. Hiseh, *ibid.*, 1990, 67, 2119
33. M.G.J. Veprek-Heijman, D. Bontand, *J. Electrochem. Soc.*, 1991, 138, 2042
34. T.B. Gorczya, Gorowitz, *VLSI Electronic Microstructure Science*, 1984, 8, 69
35. W.A.P. Claasen, et al., *J. Electrochem Soc.*, 1981, 132, 893
36. P.W. Bohn, R.C. Manz, R.C., *J. Electrochem. Soc.*, 1985, 132, 1981
37. S. Hasegawa, Y. Amano, T. Inokuma, Y. Kurata, *J. Appl. Phys.*, 1992, 72 (12) 5676
38. C.M. Drum, M.J. Rand, *J. Appl. Phys.*, 1968, 39 (9) 4458
39. L. Zambov, G. Peev, V. Shanov, S. Drumeva, *ibid.*, 1992, 43, 227

40. J.T. Cotler, J. Chapple-Sokol, *J. Electrochem. Soc.*;140 (7) ,1993
41. A.C. Adams, C.D. Capiro, *J. Electrochem. Soc.*, 1979, 126, 1042
42. J.W. Sadowski, SPIE Vol 954, *Optical Testing and Metrology*, 1988
43. M.T. Flanagan, A.N. Sloper, R.H. Ashworth, *Anal. Chem. Act.*,1988, 23
44. W.Lukosz, D. Clerc, M.Ph. Nellen, Ch. Stamm, P. Weiss, *Biosensors & Bioelectronics*,1991, 227
45. J.S. Schultz, *Scientific Amer.*, 1991, 64
46. S. Valette, S. Renard, J.P. Jadot, P. Gidon, C. Erbeia, *Sensors and Actuators*, 1990., 1087
47. N. Hartman, *R & D Magazine*, 1990., 13
48. R.G. Heideman, R.P.H. Kooyman, J. Greve, *Sensors & Actuators*, B, 1991, 4, 297
49. W. Lukosz, C.H. Stamm, *Sensors & Actuators*, A25-A27, 1991, 185
50. Boiarski,R.W. Ridgway, J.R. Busch, G. Turhan-Sayan, L.S. Miller, L.S., SPIE paper, *Chemical, Biochemical, and Environmental Fibre Sensors*, 1991
51. Y. Yamada, M. Kawachi, M. Yasu, Kobayashi, *Appl Phy. Letters*, 1984, 313
52. Pigram et. al., *Optical Engineering*, 1994., 33 B, 2594
53. E.J. Murphy, T.C. Rice, *IEEE J of Quantum Electronics.*, 1986, 928
54. A.C. Adams, S.P. Murarka, *J.Electrochem. Soc.*, 1979, 334
55. Vijayalakshmi Venkatesan., " Low Pressure Chemical Vapor Deposition of Silicon dioxide and Phosphosilicate glass Thin Films.", MS. Thesis, Dept. of Matl. Sci. & Engg., Oct 1996, MS New Jersey Institute of Technology, Newark.
56. Sung Jun Lee, "Synthesis and Charaterization of silicon do oxide thin films by LPCVD using DTBS and oxygen ", MS thesis, Dept. of Matl. Sci. & Engg, Oct 1996, New Jersey Institute of Technology, Newark